4th BIG meeting @ UB

# Constraining Primordial Black Holes with Gravitational Waves


Sachiko Kuroyanagi

IFT UAM-CSIC / Nagoya University


29 Nov 2024

# Gravitational wave (GW) observation

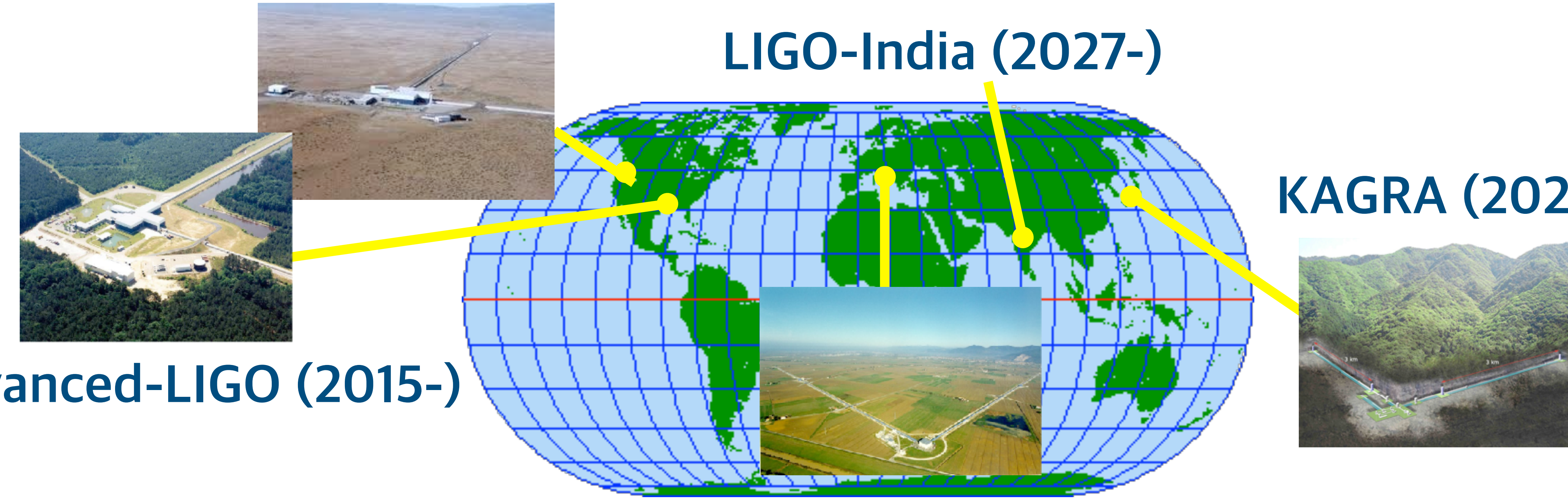


2015 — 2020' — 2030'

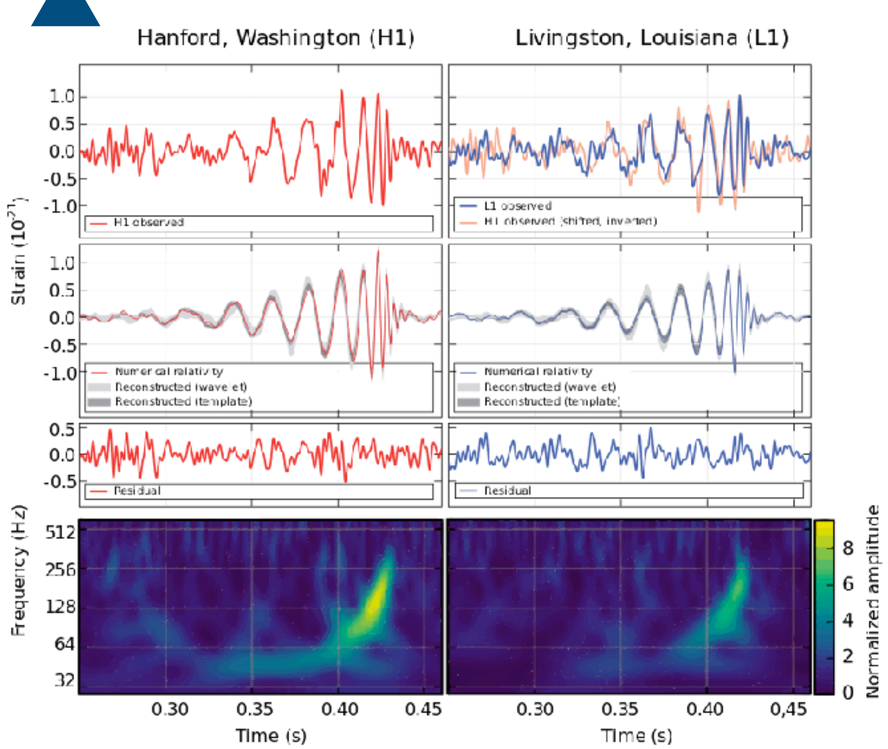


The first detection: GW150914

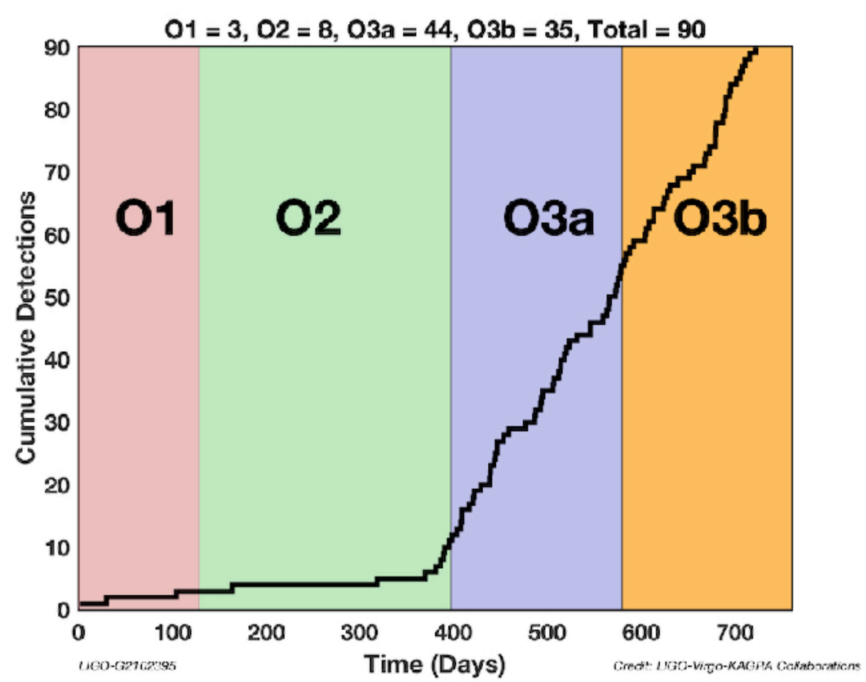


O4 started in May 2023

## Future projects

- Einstein Telescope

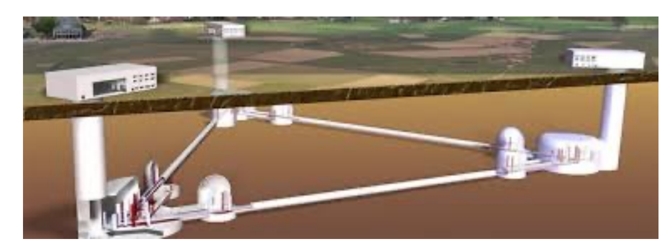

- Cosmic Explorer

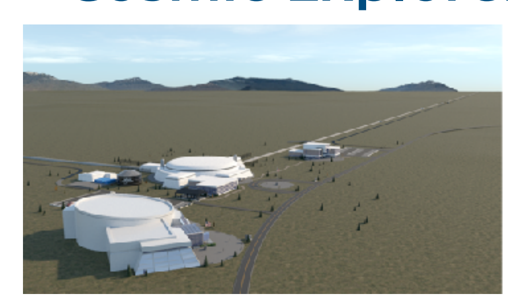

etc.

# Primordial Black Holes (PBHs)

**= Black holes generated in the early universe**

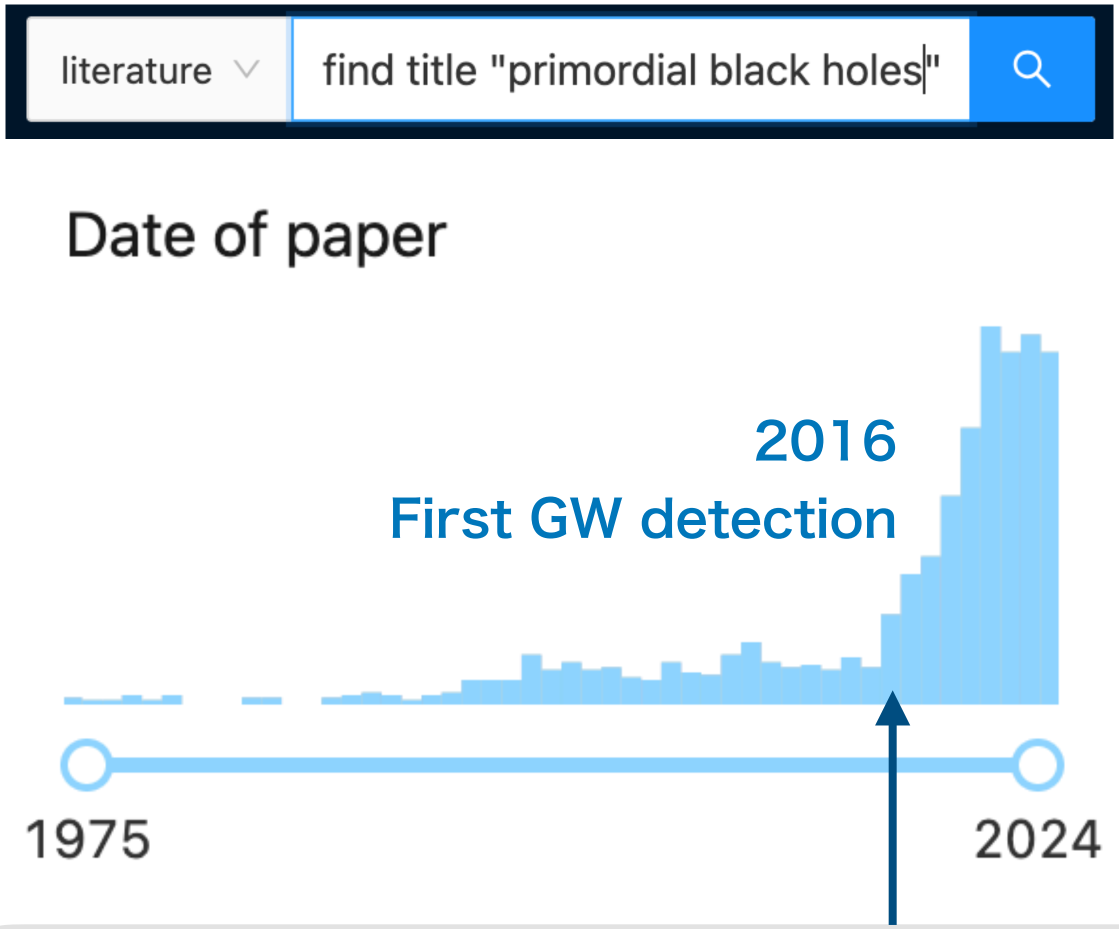


could originate from

- **Inflation**
- Reheating
- Phase transitions
- Collapse of cosmic strings
- Scalar field instabilities

etc.

**Origin of the observed 30 $M_\odot$ BBHs could be primordial.**

Bird et al., PRL 116, 201301 (2016)
Clesse & Garcia-Bellido, PDU 10, 002 (2016)
Sasaki et al., PRL 117, 061101 (2016)

# GWs as a probe of PBHs

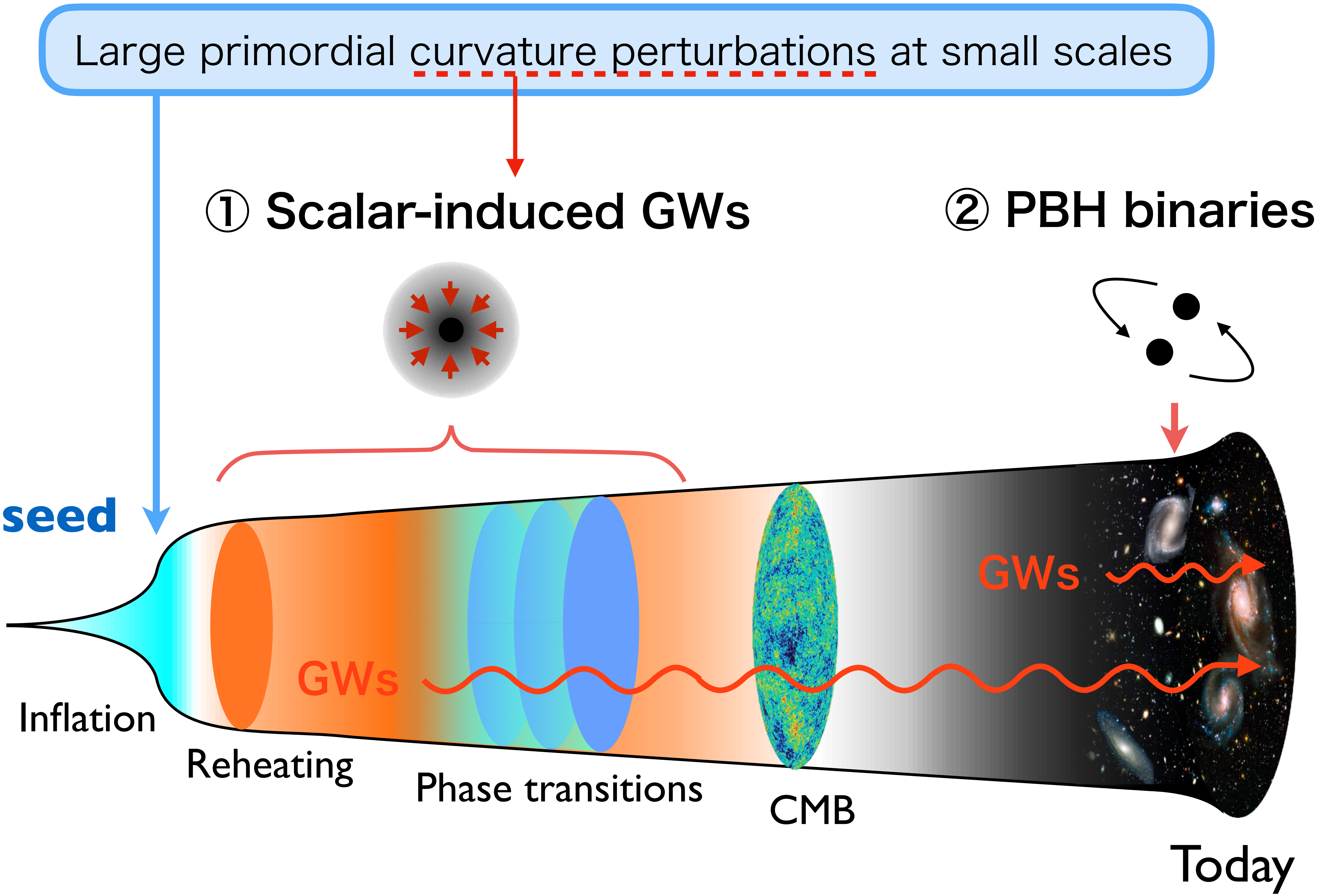

# Various ways to search PBHs

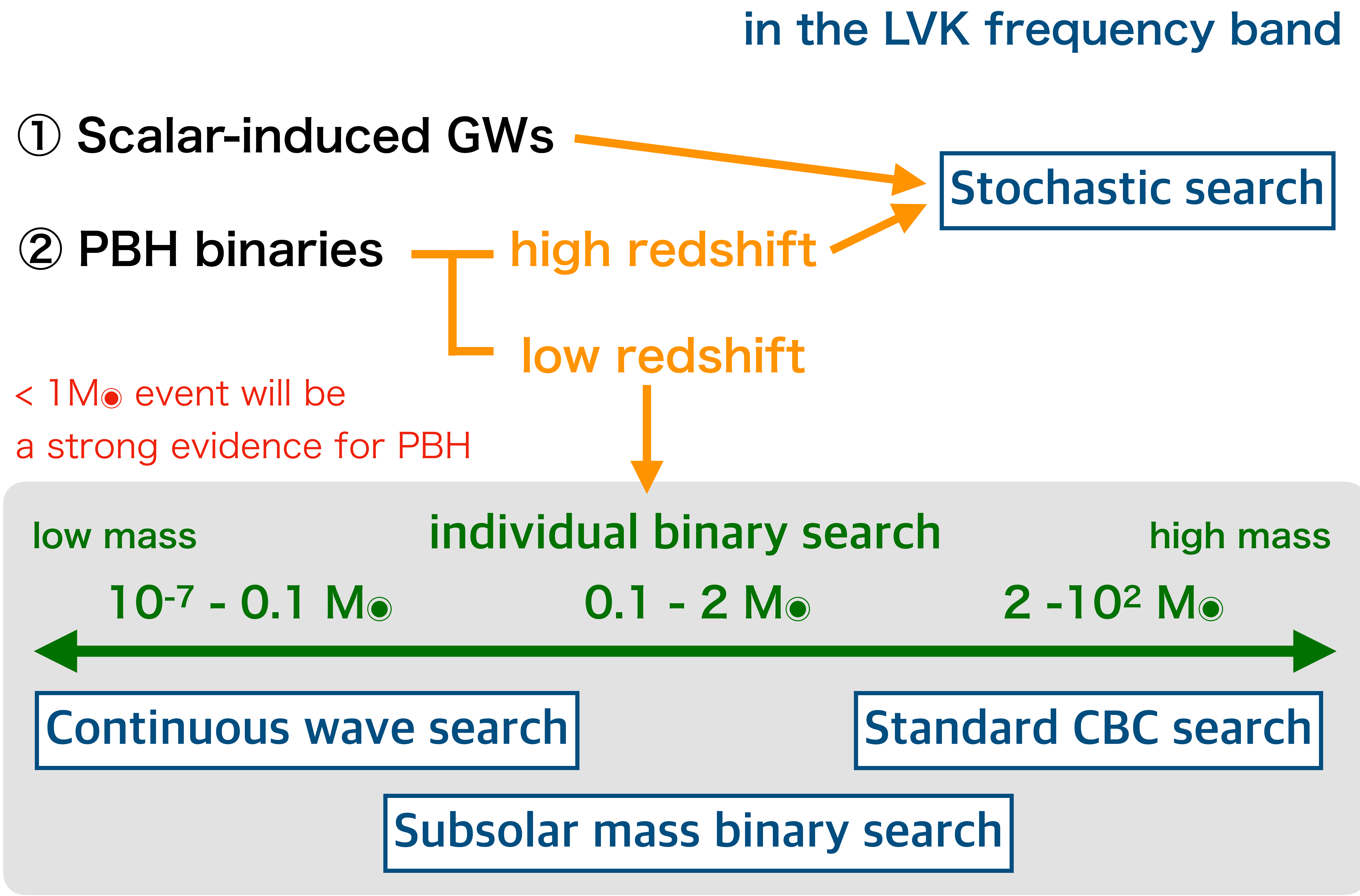

# Stochastic GW background search

# GW background as a probe of the early universe!

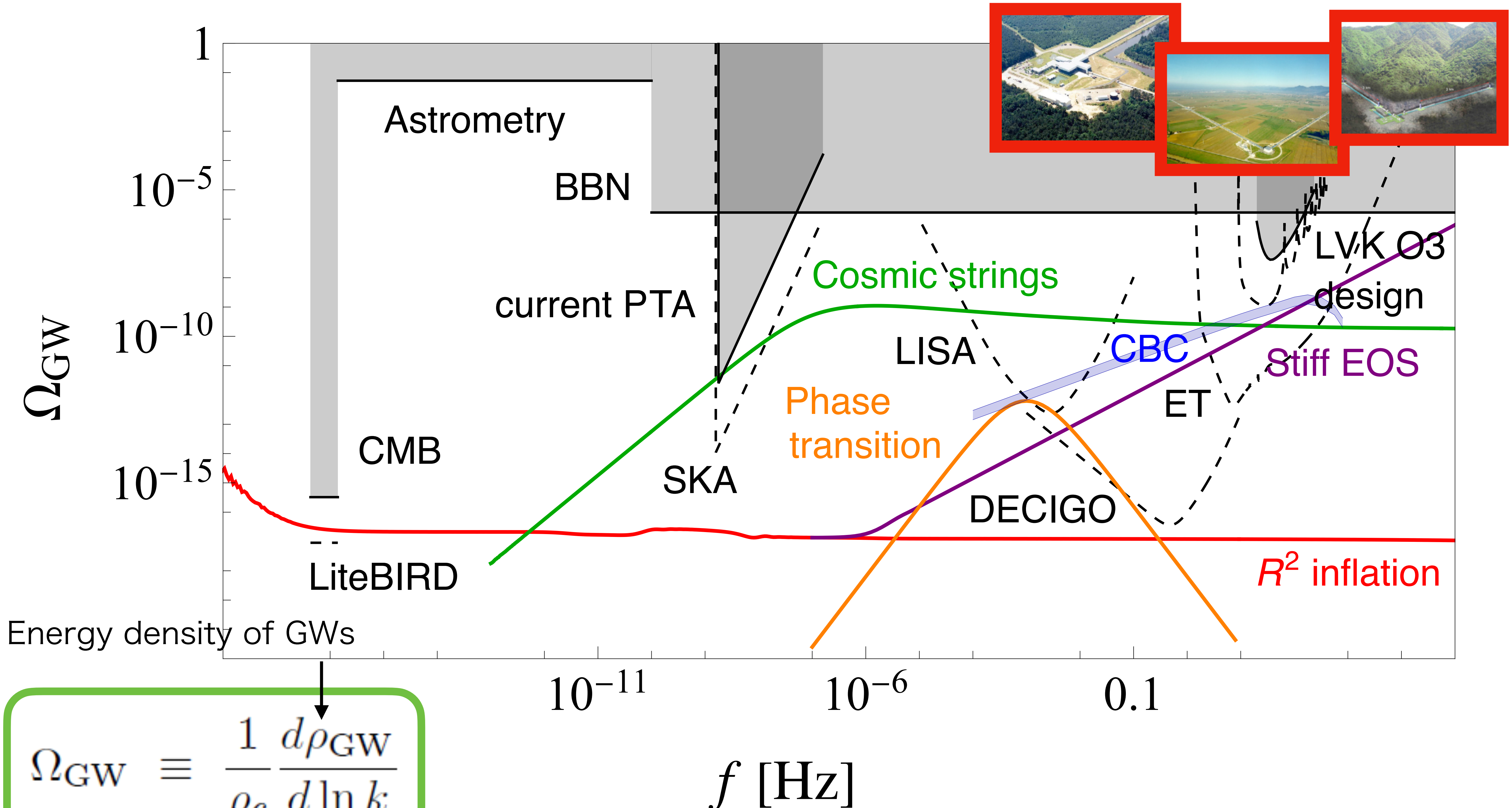


Energy density of GWs

$$\Omega_{\rm GW} \equiv \frac{1}{\rho_c}\frac{d\rho_{\rm GW}}{d\ln k}$$

Critical density of the Universe

→ **a unique test of high energy theories**

# Scalar-induced GWs

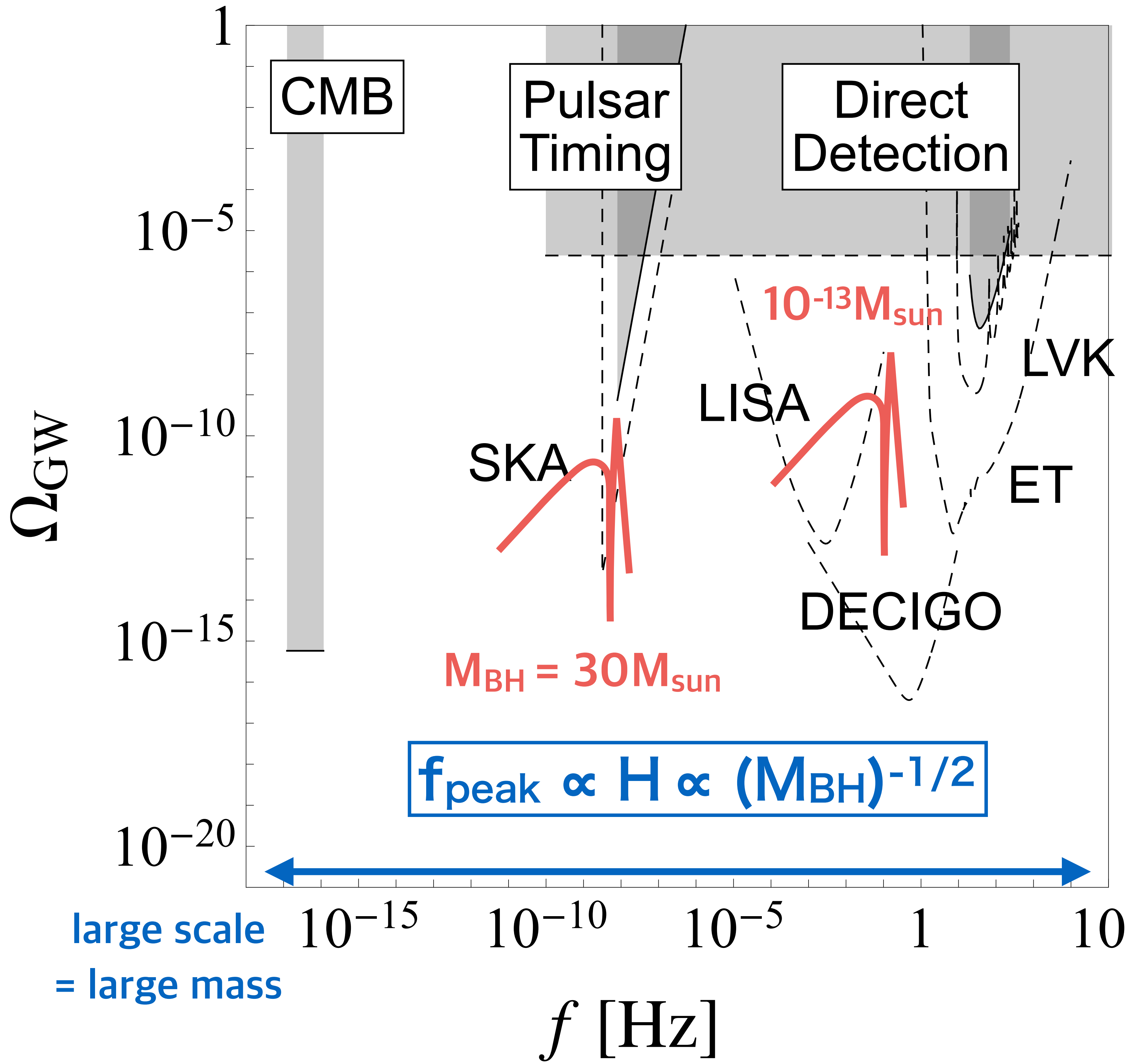


GWs are generated associated with **PBH formation** in the RD era

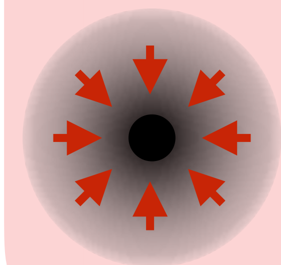

$$\mathcal{P}_{\Psi}(k) = \mathcal{A}^2 \delta_D(\ln(k/k_p))$$

δ function peak is assumed

R. Saito & J. Yokoyama, PRL 102, 161101 (2009)

# Scalar-induced GWs

Evolution equation for GWs

$$h''_{ij} + 2\mathcal{H}h'_{ij} - \nabla^2 h_{ij} = -4\hat{\mathcal{T}}_{ij}{}^{lm}\mathcal{S}_{lm}$$

source term $\Phi \equiv \Phi^{(1)}, \ \Psi \equiv \Psi^{(1)}$

$$\begin{aligned}\mathcal{S}_{ij} \equiv\ & 2\Phi\partial^i\partial_j\Phi - 2\Psi\partial^i\partial_j\Phi + 4\Psi\partial^i\partial_j\Psi + \partial^i\Phi\partial_j\Phi \\ & - \partial^i\Phi\partial_j\Psi - \partial^i\Psi\partial_j\Phi + 3\partial^i\Psi\partial_j\Psi \\ & - \frac{4}{3(1+w)\mathcal{H}^2}\partial_i(\Psi' + \mathcal{H}\Phi)\partial_j(\Psi' + \mathcal{H}\Phi) \\ & - \frac{2c_s^2}{3w\mathcal{H}^2}[3\mathcal{H}(\mathcal{H}\Phi - \Psi') + \nabla^2\Psi]\partial_i\partial_j(\Phi - \Psi)\end{aligned}$$

2nd order of scalar perturbations

$$ds^2 = a^2(\eta)[-(1+2\underline{\Phi})d^2\eta + [(1-2\underline{\Psi})\delta_{ij} + h_{ij}]dx^i dx^j]$$

# GWs from PBH mergers

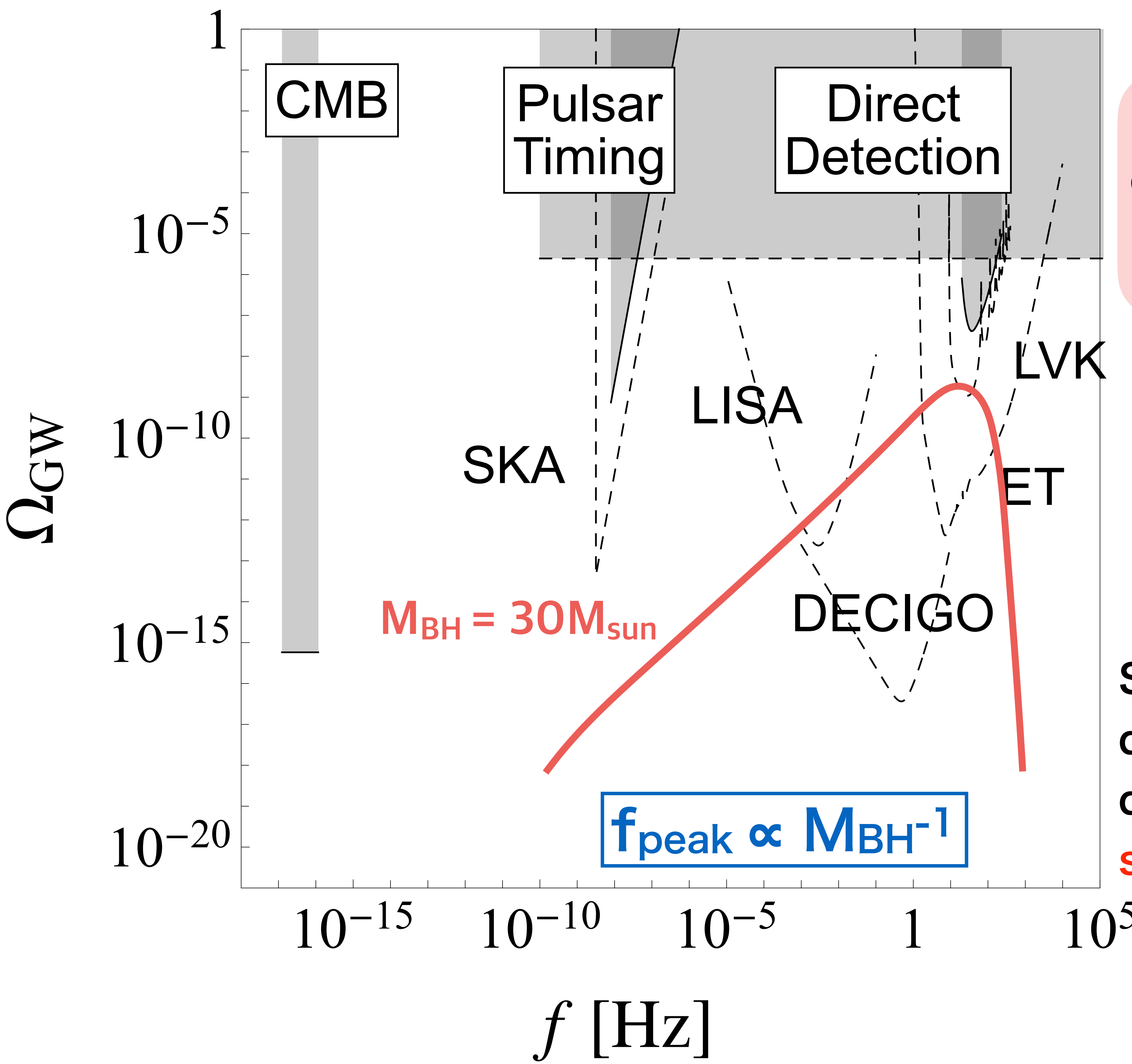


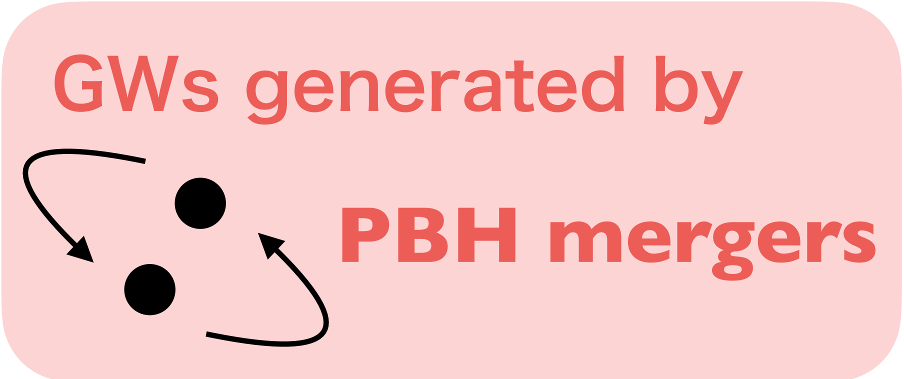


Superposition of distant events are detectable as a stochastic GW background

S. Clesse & J. García-Bellido, Phys. Dark Univ. 18, 105 (2017)

# Expected constraints

for monochromatic mass function

with threshold of SNR = 8

## ① Scalar-induced GWs

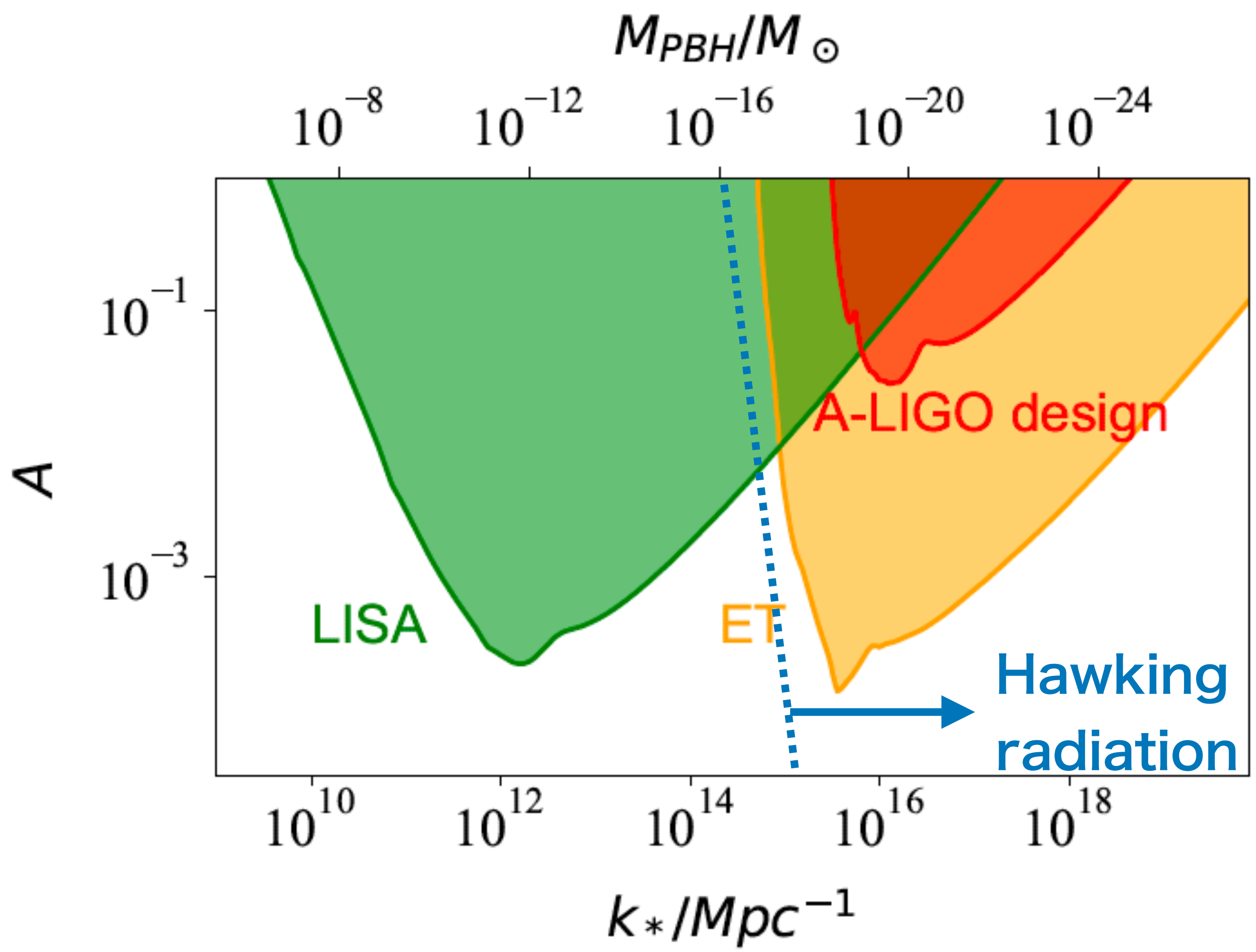


## ② PBH mergers

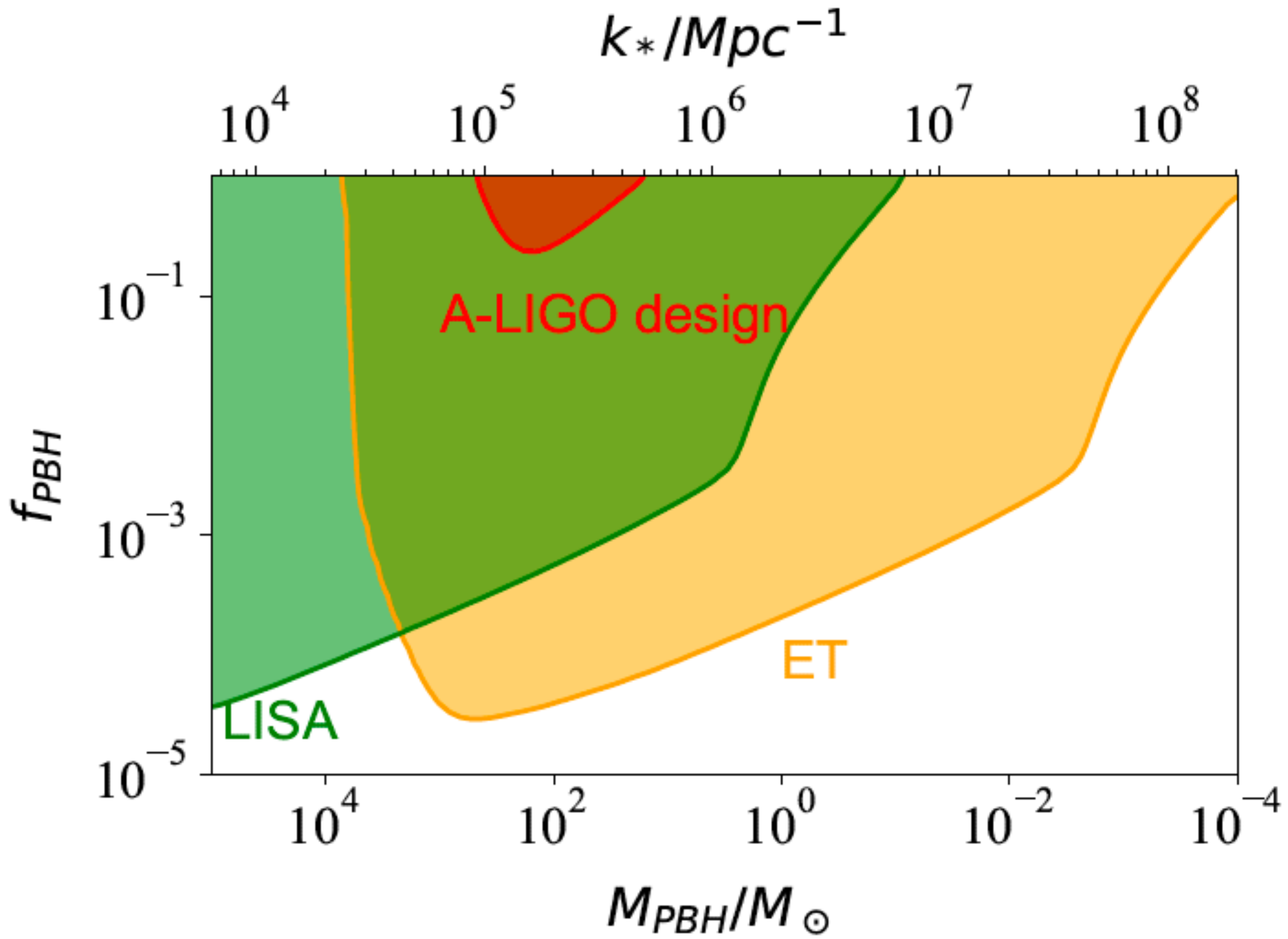


→ can be avoided if BH has longer lifetime
(possible with quantum effects?)


V. Thoss et al., MNRAS 532, 1, (2024) 451-459
K. Kohri et al., arXiv:2409.06365

# Spectrum for broad mass function

lognormal mass function with width Δ

## ① Scalar-induced GWs

peak scale of curvature perturbation

$f \propto k_{peak} \propto M_{PBH}^{-1/2}$

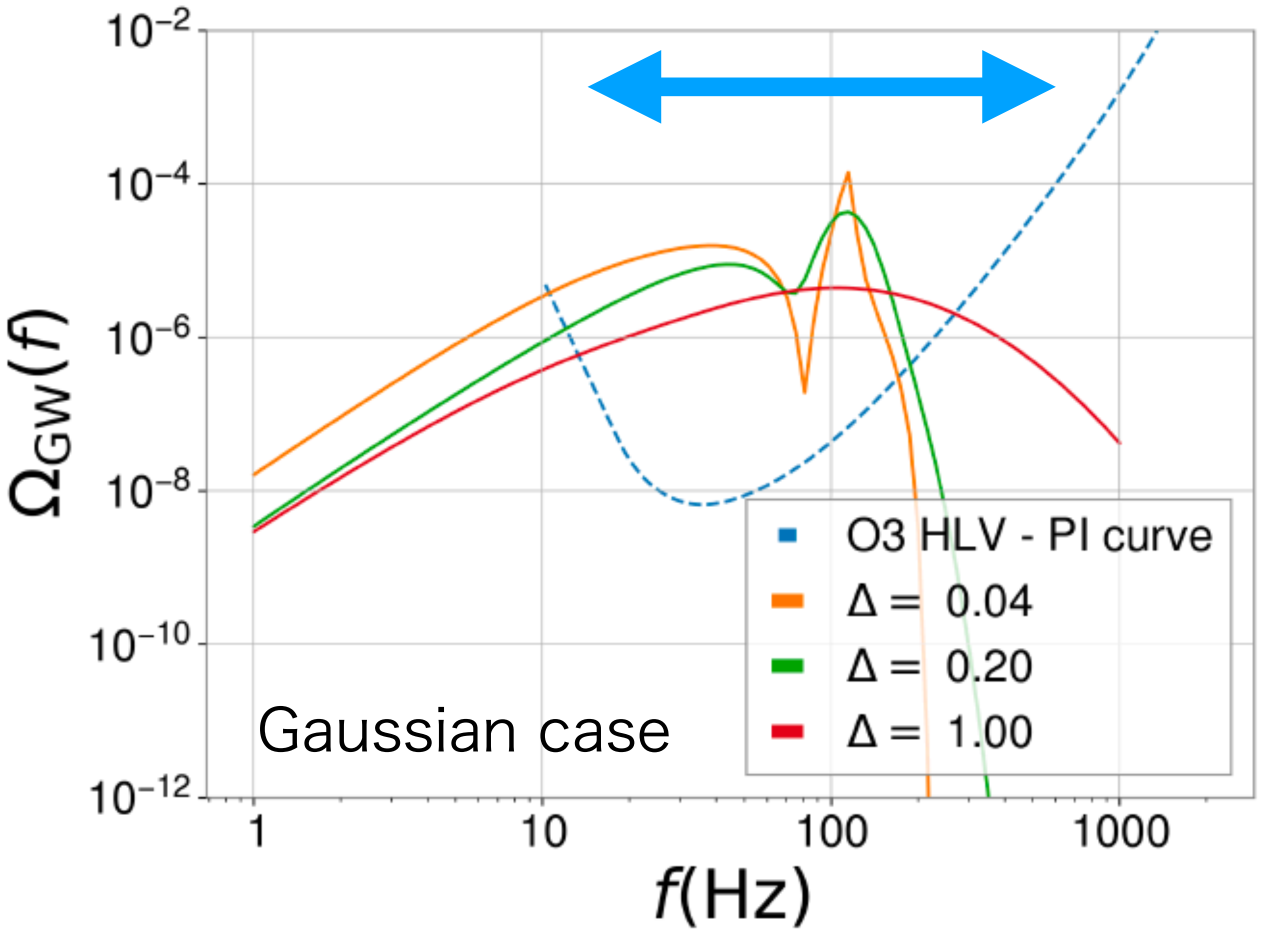


## ② PBH mergers

PBH mass

$f \propto M_{PBH}^{-1}$

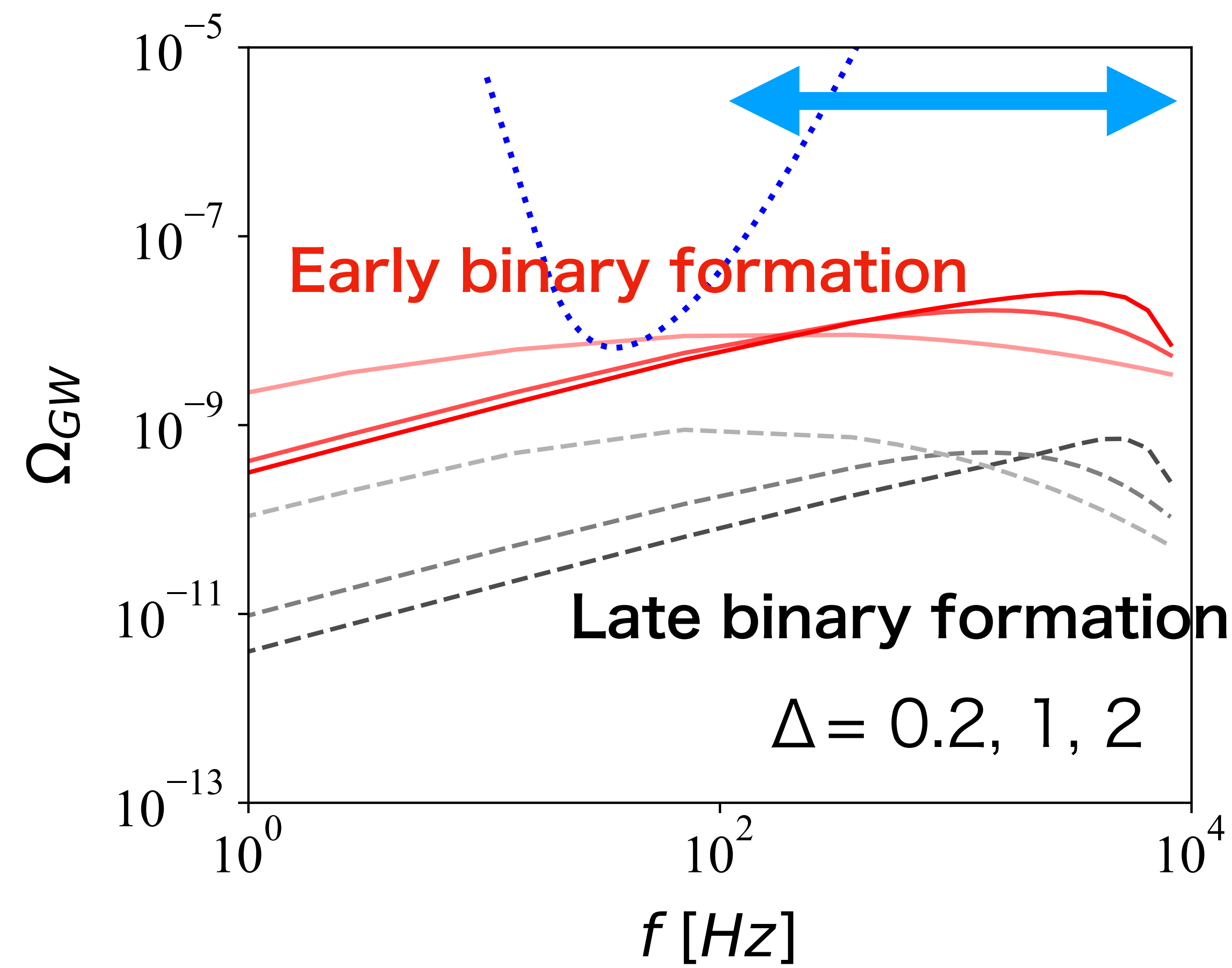

# How to provide a constraint from LVK data

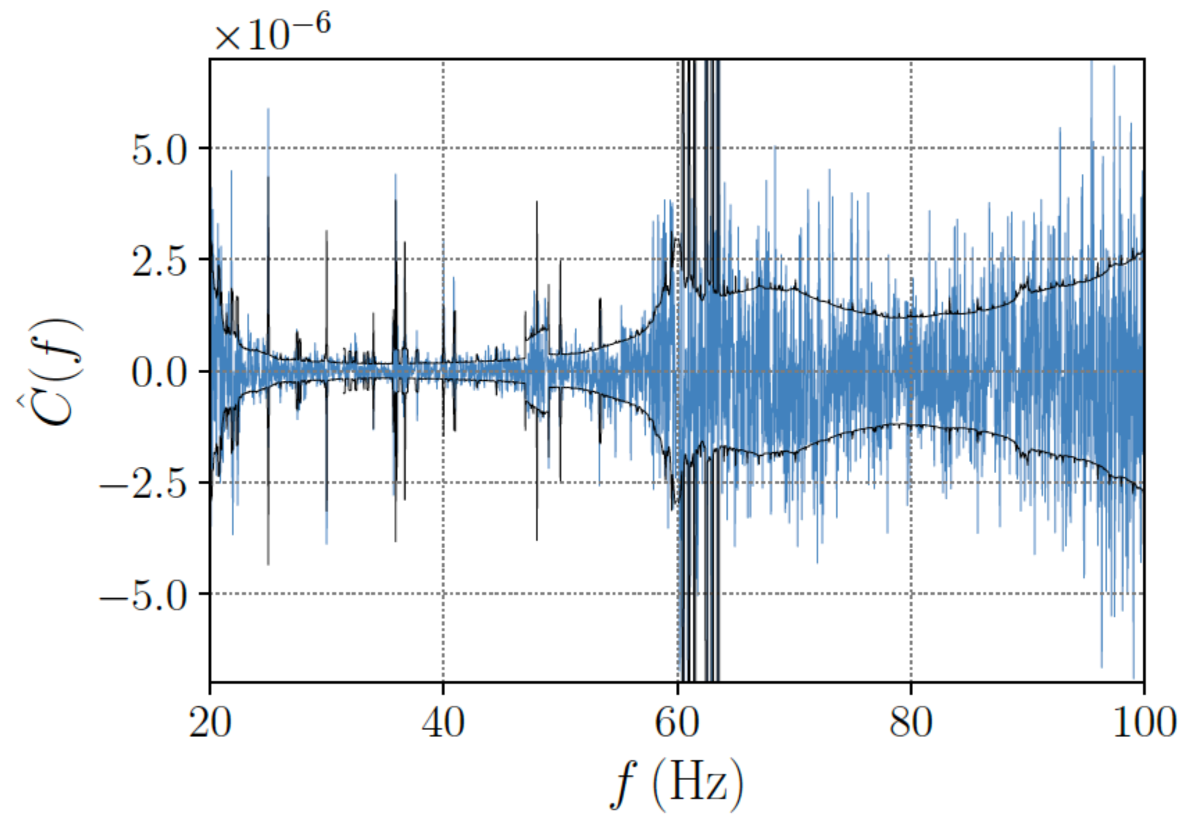


Data is available at https://dcc.ligo.org/LIGO-G2001287/public

## pygwb

**Open access Python module published from the LVK collaboration for a stochastic background analysis**

Renzini et al., ApJ 952, 25 (2023)
https://pypi.org/project/pygwb/
see also https://pygwb.docs.ligo.org/pygwb/

pygwb 1.5.1

```
pip install pygwb
```

# How to detect a stochastic background

**Cross Correlation**

detector1

$$s_1(t) = h(t) + n_1(t)$$

detector2

$$s_2(t) = h(t) + n_2(t)$$

s: observed signal
h: gravitational waves
n: noise

$$\langle S\rangle = \int_{-T/2}^{T/2} dt\ \langle s_1(t)s_2(t)\rangle$$

$$= \int_{-T/2}^{T/2} dt\ \langle h^2(t) + \underline{h(t)n_2(t) + n_1(t)h(t) + n_1(t)n_2(t)}\rangle$$

no correlations $\rightarrow 0$

$$= \int_{-T/2}^{T/2} dt\ \underline{\langle h^2(t)\rangle}$$

GW signal

(for detectors at the same location)

# What we do in the LVK stochastic search

Renzini et al., ApJ 952, 25 (2023)

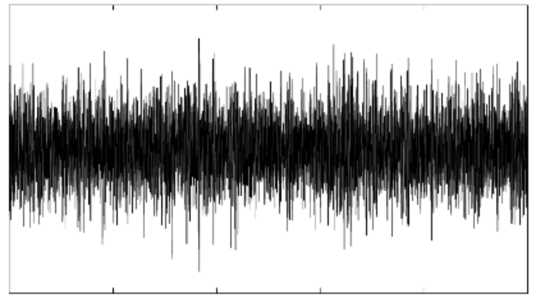

strain data 1

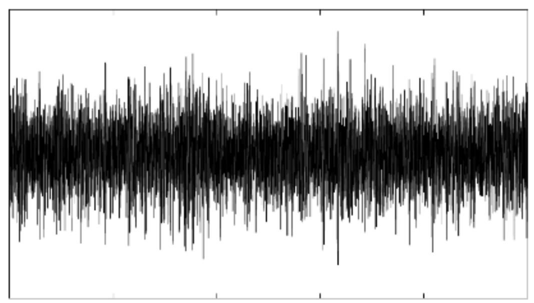

strain data 2

**strain data in discrete Fourier space**

$$\tilde{s}_f \equiv \sum_{t_k=0}^{T-\delta t} s(t_k)\, e^{-i2\pi m t_k/T}$$

for every T = 192 s

**cross-correlated spectrum**

$$C_{IJ,f} = \frac{2}{T}\tilde{s}^*_{I,f}\tilde{s}_{J,f}$$

IJ: detector combinations

**estimator**

$$\hat{\Omega}_{\mathrm{GW},f} = \frac{\mathrm{Re}[C_{IJ,f}]}{\gamma_{IJ}(f)\, S_0(f)}$$

$$S_0(f) = \frac{3H_0^2}{10\pi^2}\frac{1}{f^3}$$

c.f. $g_{ab} = \eta_{ab} + h_{ab}$

$$\langle h_{ab}(t)h^{ab}(t)\rangle = 2\int_{-\infty}^{\infty} \mathrm{d}f\, S_h(f)$$

$$\Omega_{\mathrm{gw}}(f) = (4\pi^2/3H_0^2) f^3 S_h(f)$$

**overlap reduction function**

takes into account
the detector's locations and orientations

# Overlap reduction function

Detectors are located at different site and facing different direction

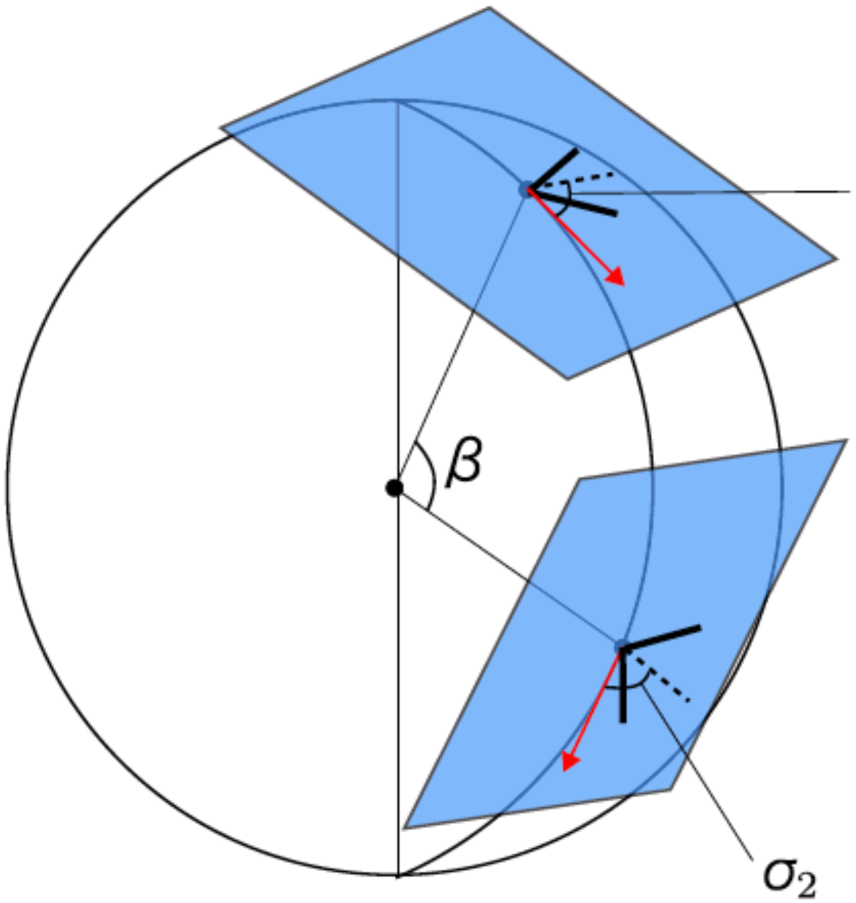


① Time difference

② Antenna pattern

+ mode

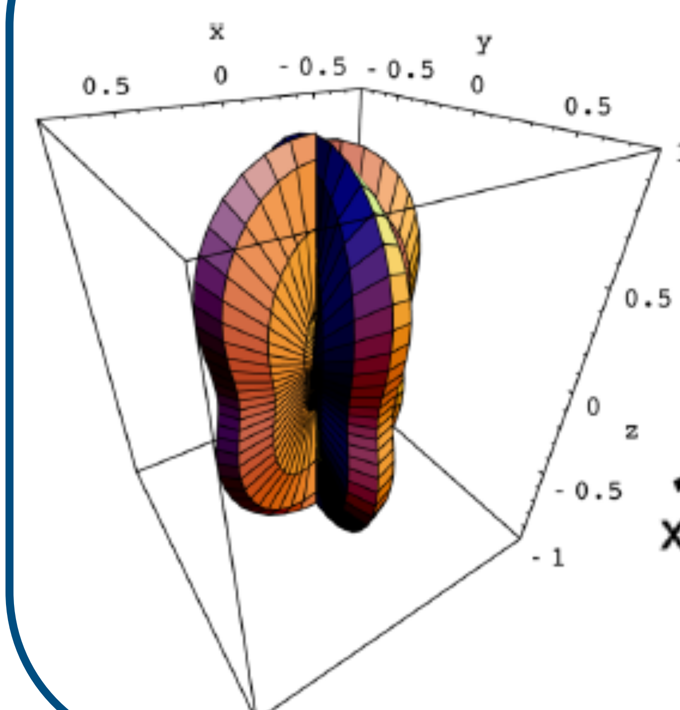

× mode

detector arms

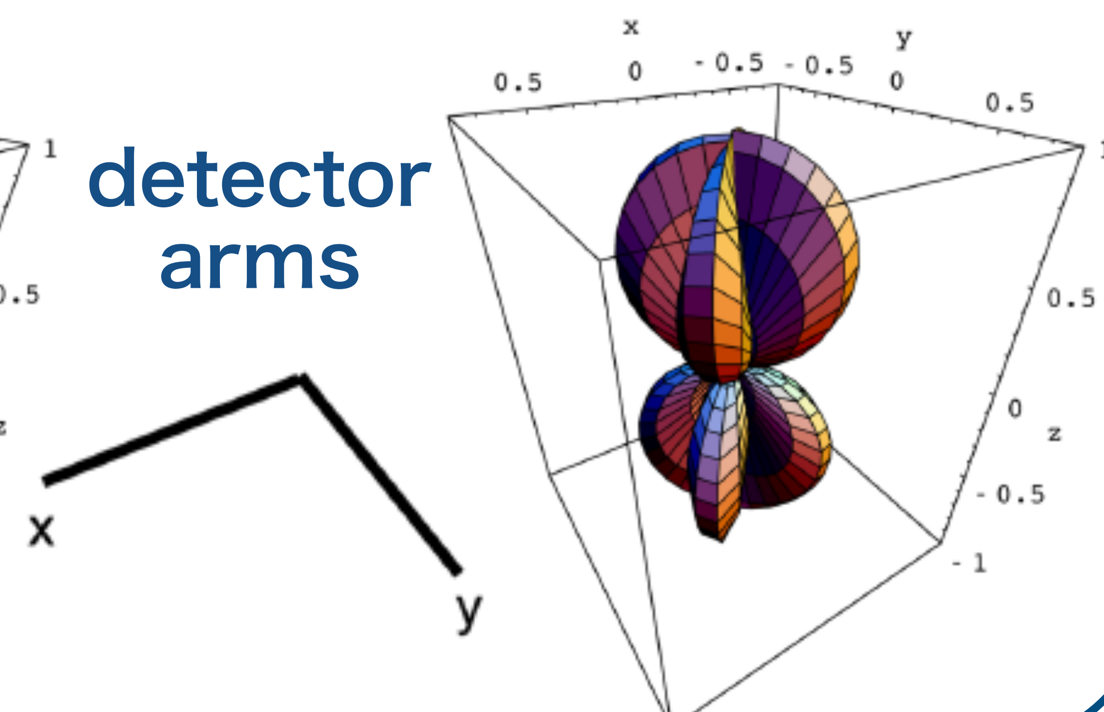


Figure from A. Nishizawa et al. PRD 79, 082002 (2009)

# Variance: level of noise

**strain data in discrete Fourier space**

signal ↓ noise ↓

$$\tilde{s}_{I,f} = F_I \tilde{h}_f + \tilde{n}_{I,f}$$

↑ antenna pattern for + and x → gives $\gamma_{IJ}(f)$

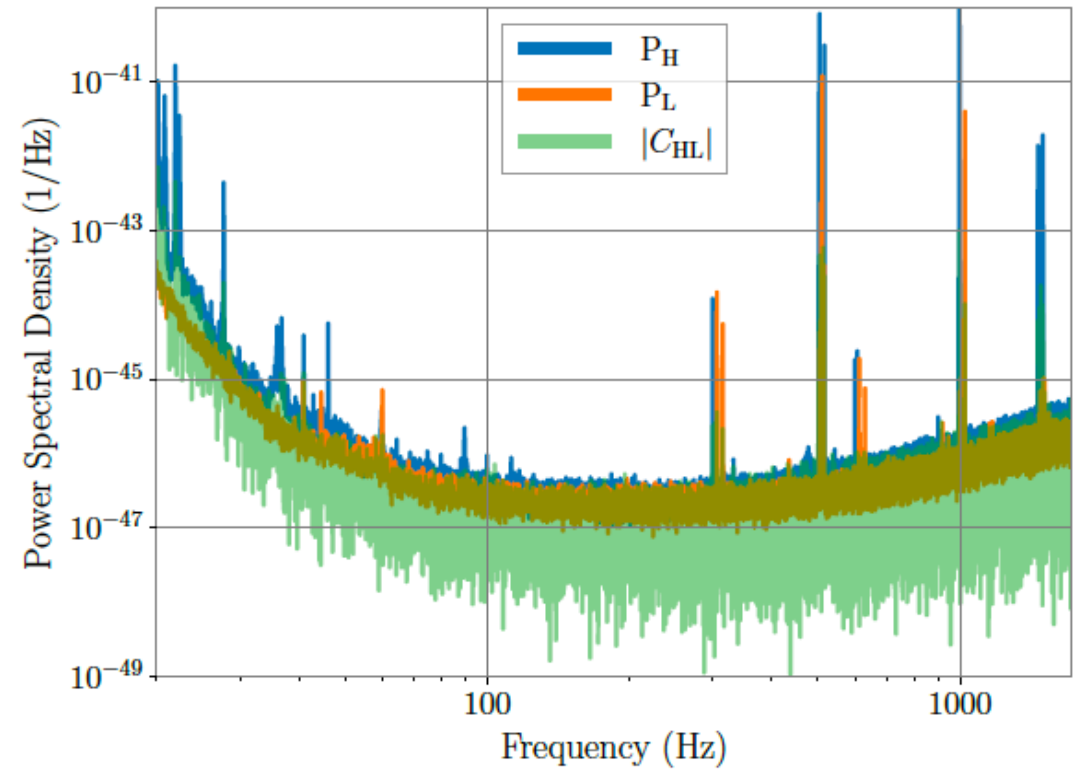


**cross-correlation**

$$C_{IJ,f} = \frac{2}{T} \tilde{s}^*_{I,f} \tilde{s}_{J,f}$$

→ dominated by $\langle \tilde{h}_f^2 \rangle$ signal

**estimator**

$$\hat{\Omega}_{\mathrm{GW},f} = \frac{\mathrm{Re}[C_{IJ,f}]}{\gamma_{IJ}(f) S_0(f)}$$

**auto-correlation**

$$P_{I,f} = \frac{2}{T} |\tilde{s}_{I,f}|^2$$

→ dominated by $\langle \tilde{n}_{I,f}^2 \rangle$ noise

**variance**

$$\sigma^2_{IJ,k} = \frac{1}{2T\Delta f} \frac{P_{I,f} P_{J,f}}{\gamma^2_{IJ}(f) S_0^2(f)}$$

→ an indicator of the level of noise

# Likelihood analysis

data (cross-correlated spectrum)

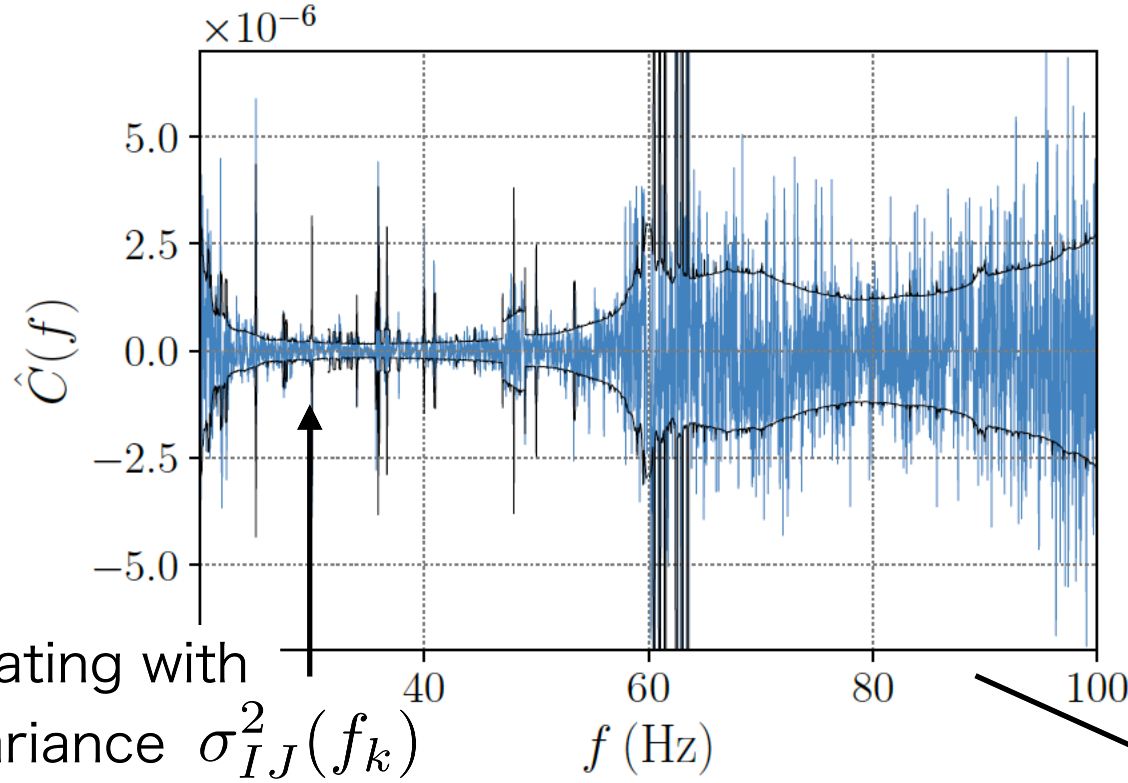


fluctuating with the variance $\sigma^2_{IJ}(f_k)$

Your model

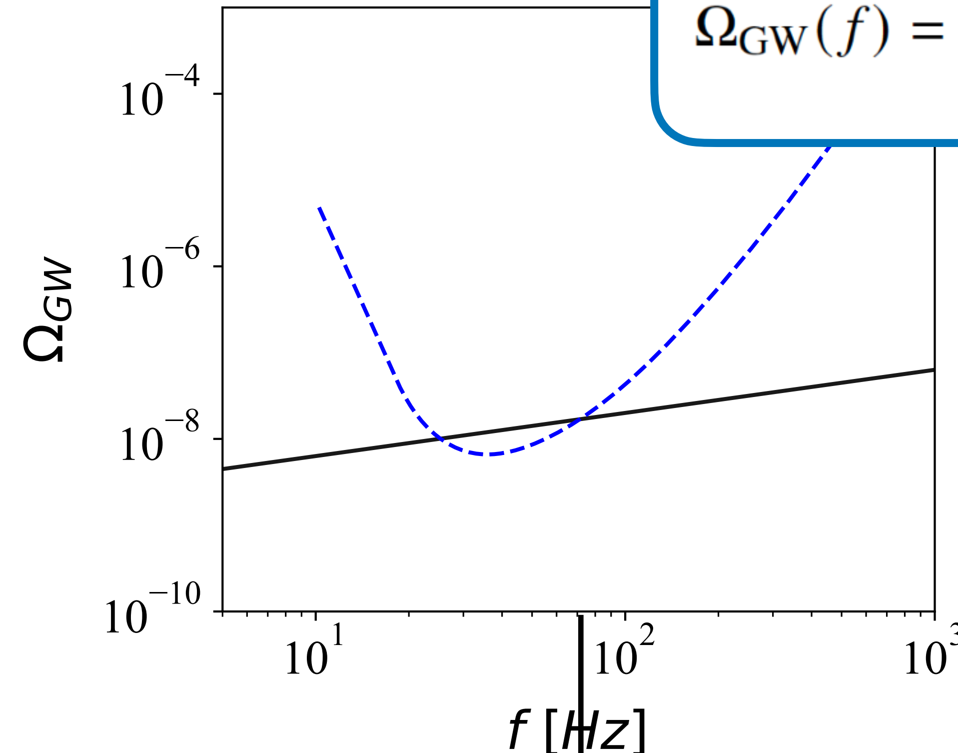


LVK analysis

**Model = power-law**

$$\Omega_{\rm GW}(f) = \Omega_\alpha \left(\frac{f}{f_{\rm ref}}\right)^\alpha$$

**Likelihood**

$$p(\hat{C}_k^{IJ}|\mathbf{\Theta}) \propto \exp\left[-\frac{1}{2}\sum_{IJ}\sum_k \left(\frac{\hat{C}_k^{IJ} - \Omega_{\rm M}(f_k|\mathbf{\Theta})}{\sigma^2_{IJ}(f_k)}\right)^2\right]$$

variance

IJ: detector combinations

k: frequencies

Prior

**Posterior distribution**

$$p(\mathbf{\Theta}|C_k^{IJ}) \propto p(C_k^{IJ}|\mathbf{\Theta})p(\mathbf{\Theta})$$

# Likelihood analysis

Posterior distribution $\propto$

$$p(\hat{C}_k^{IJ}|\boldsymbol{\Theta}) \propto \exp\left[-\frac{1}{2}\sum_{IJ}\sum_k\left(\frac{\hat{C}_k^{IJ} - \Omega_{\rm M}(f_k|\boldsymbol{\Theta})}{\sigma_{IJ}^2(f_k)}\right)^2\right]$$

IJ: detector combinations
k: frequencies

(for a flat & infinite-range prior)

Constraint by O3 data

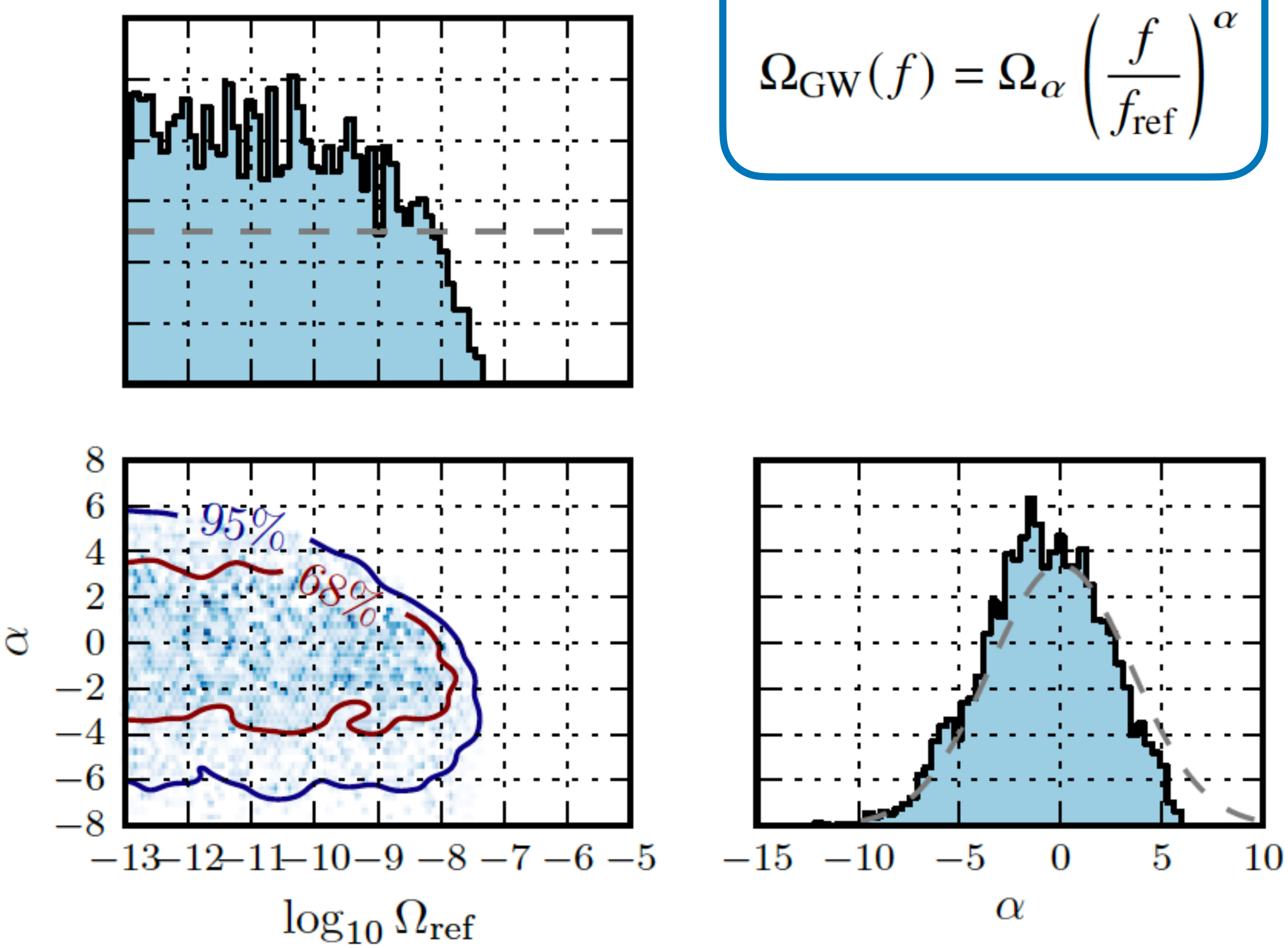


**Model = power-law**

$$\Omega_{\rm GW}(f) = \Omega_\alpha\left(\frac{f}{f_{\rm ref}}\right)^\alpha$$

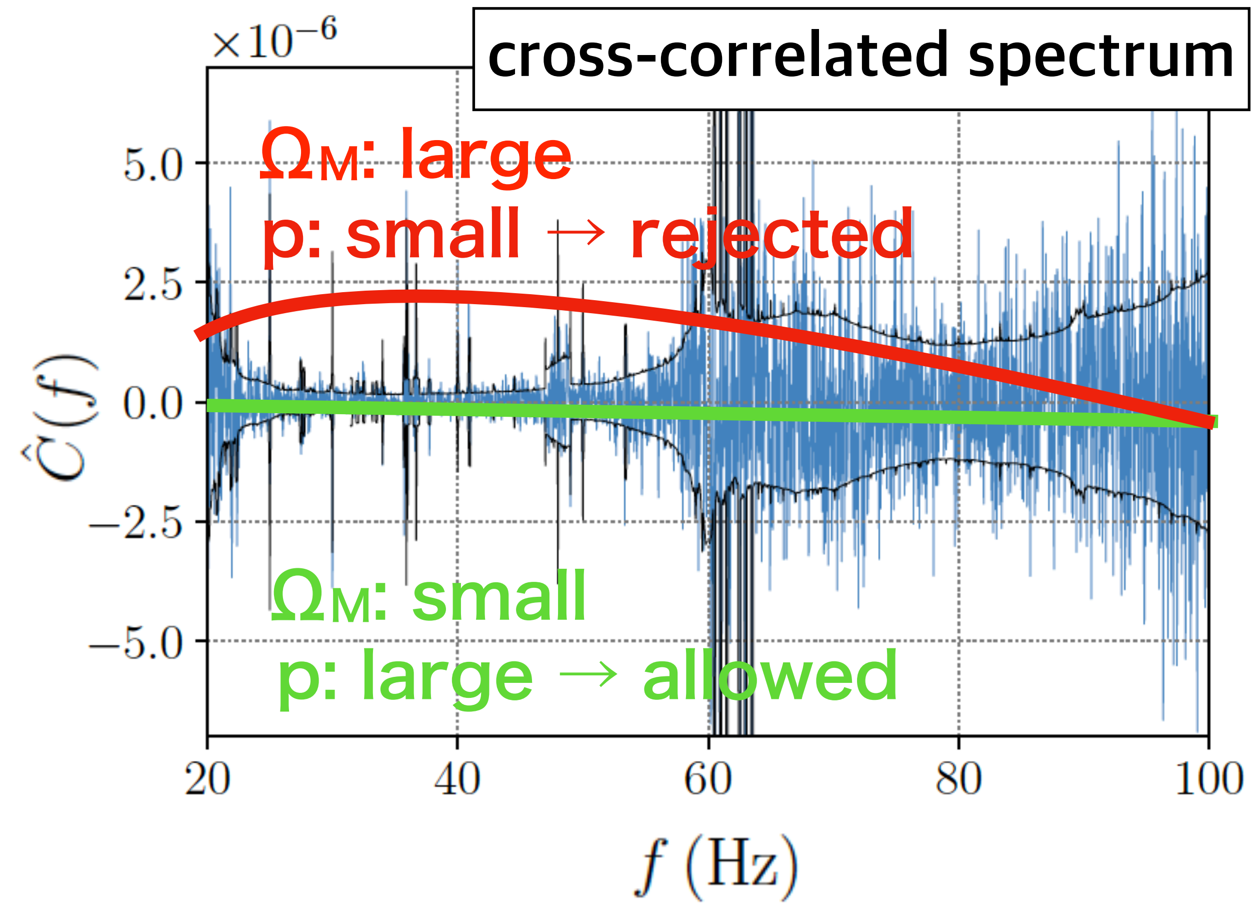


LVK collaboration, PRD 104, 022004 (2021)

# Probing GWs with features

FAQ: Can we detect features in GW background?

Likelihood

$$p(\hat{C}_k^{IJ}|\boldsymbol{\Theta}) \propto \exp\left[-\frac{1}{2}\sum_{IJ}\sum_{k}\left(\frac{\hat{C}_k^{IJ}-\Omega_{\rm M}(f_k|\boldsymbol{\Theta})}{\sigma_{IJ}^2(f_k)}\right)^2\right]$$

k: frequencies

→ Yes, features can be detected if the signal has high enough SNR (at least 1) in the corresponding frequency bin.

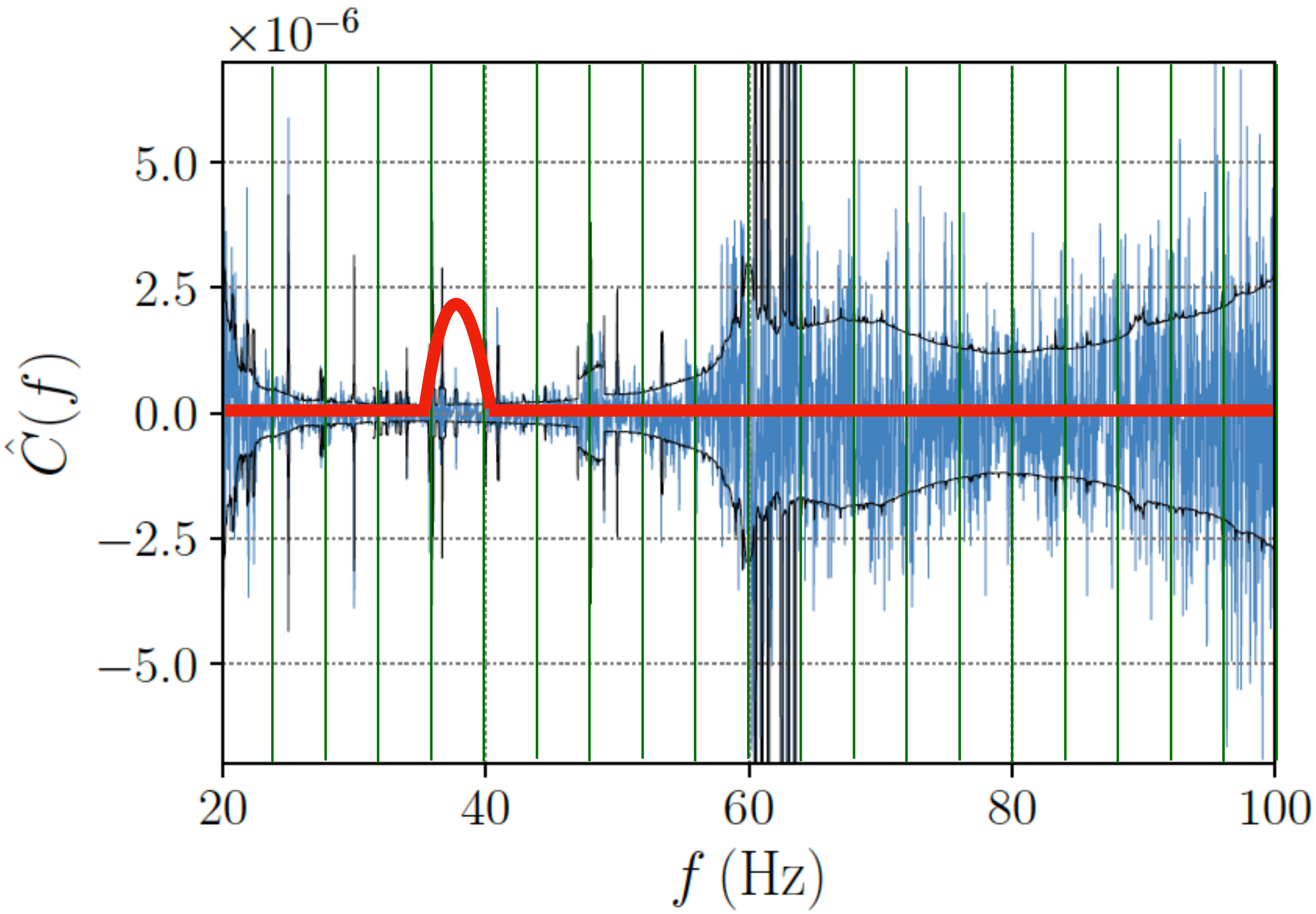


narrower bin
→ fine feature

wider bin
→ high SNR in the bin
+ stable noise estimation

LVK analysis

Frequency resolution
1/32Hz

# ① LVK O3 constraint on scalar induced GWs

GW spectrum

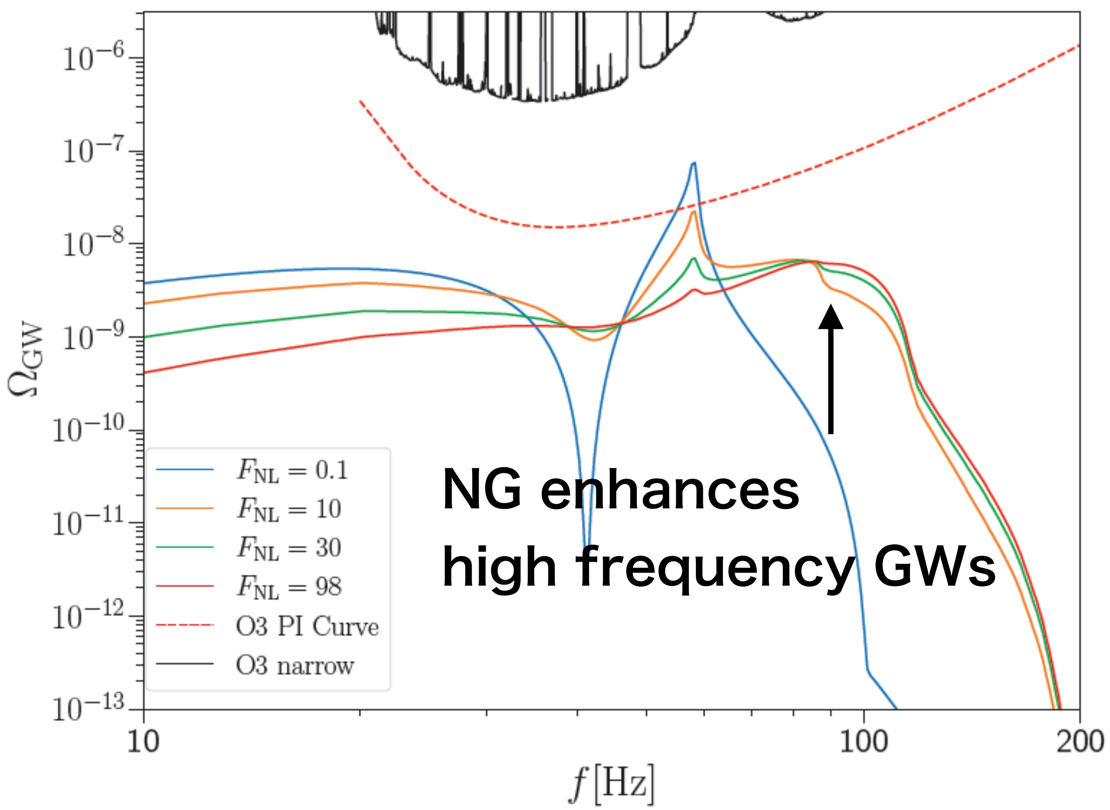


Many inflationary models predicting large curvature perturbations (and producing PBHs) exhibit Non-Gaussianity (NG)

- ultra slow roll inflation
- multi field inflation
- couplings leading to particle production, etc.

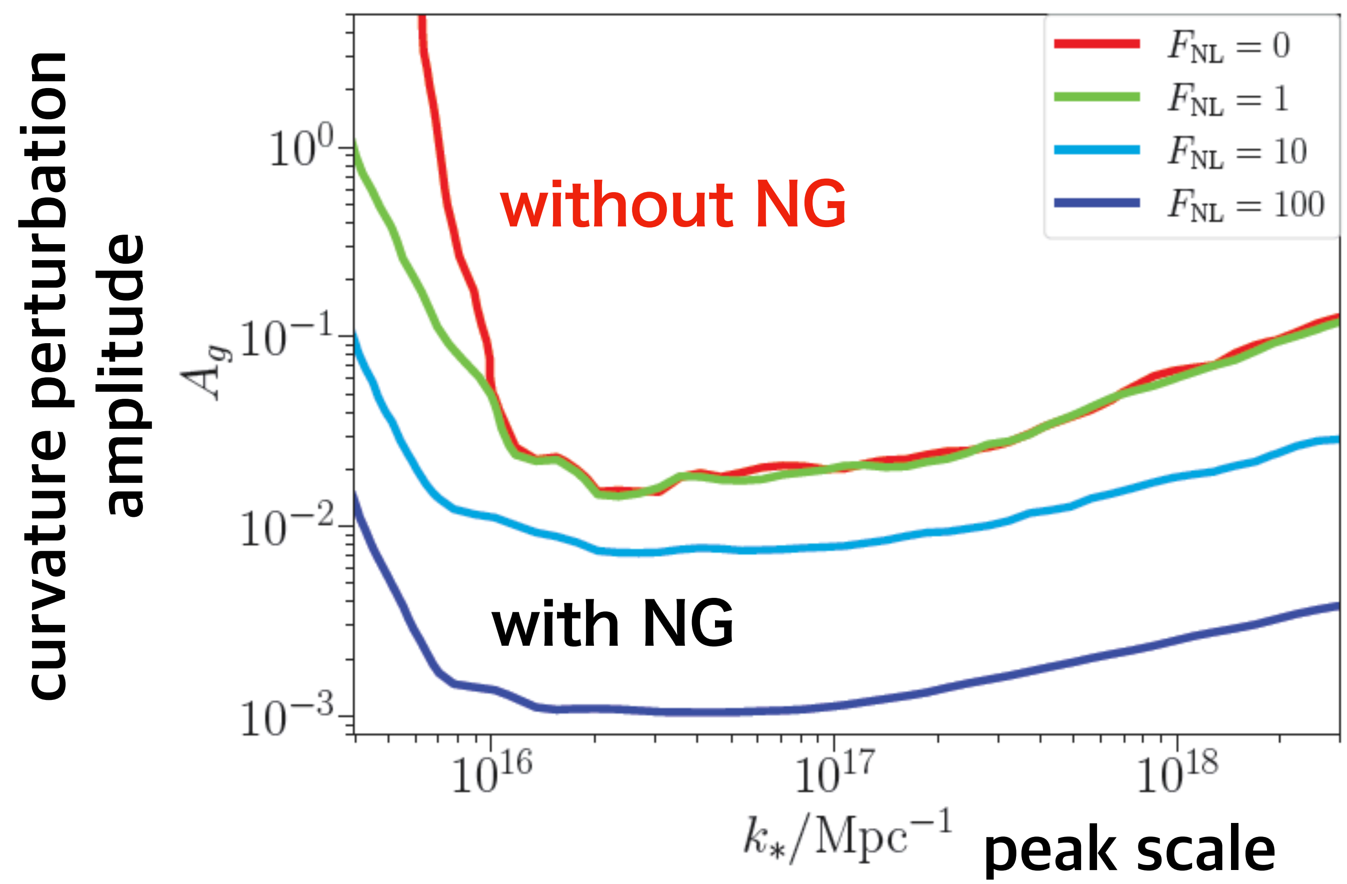


**Assumption:**
**local type non-Gaussianity**

$$\zeta(\mathbf{x}) = \zeta_g(\mathbf{x}) + F_{\rm NL}\zeta_g^2(\mathbf{x})$$

Note: Parametrization with $F_{\rm NL}$ covers limited cases

R. Inui, S. Jaraba, SK, S. Yokoyama, JCAP 05 (2024) 082

# Note on the form of non-Gaussianity

**Our assumption:**
**local type non-Gaussianity**

$$\zeta(\mathbf{x}) = \zeta_g(\mathbf{x}) + F_{\rm NL}\zeta_g^2(\mathbf{x})$$

perturbative expansion

**The form of non-Gaussianity can be very different**

e.g. quantum diffusion
J. M. Ezquiaga et al.,
JCAP 03 (2020) 029

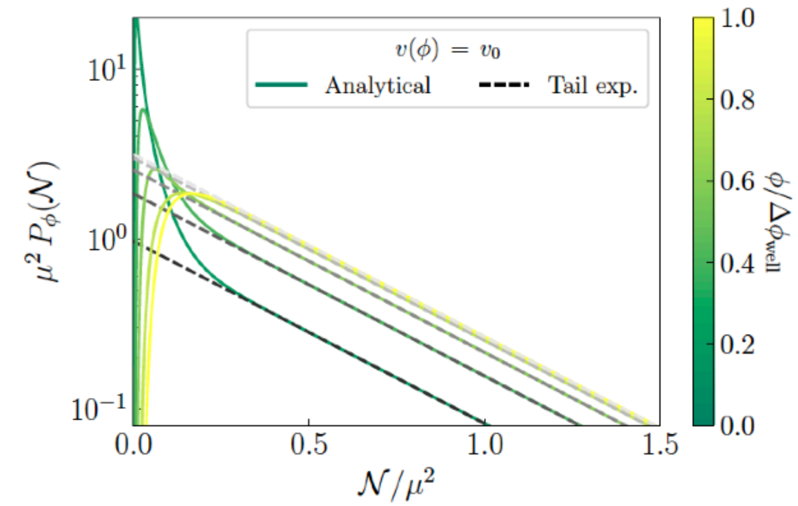


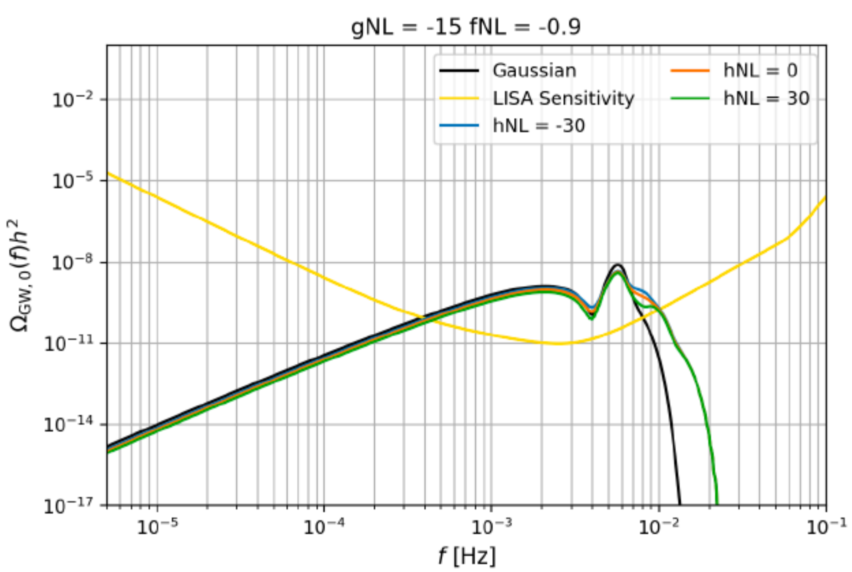


G. Perna et al., arXiv:2403.06962

**5th order non-neglible contribution?**

$$\mathcal{R}(\mathbf{x}) = \mathcal{R}_g(\mathbf{x}) + f_{\rm NL}(\mathcal{R}_g^2(\mathbf{x}) - \langle\mathcal{R}_g^2\rangle) + g_{\rm NL}\mathcal{R}_g^3(\mathbf{x}) + h_{\rm NL}(\mathcal{R}_g^4(\mathbf{x}) - 3\langle\mathcal{R}_g^2\rangle^2) + i_{\rm NL}\mathcal{R}_g^5(\mathbf{x})$$

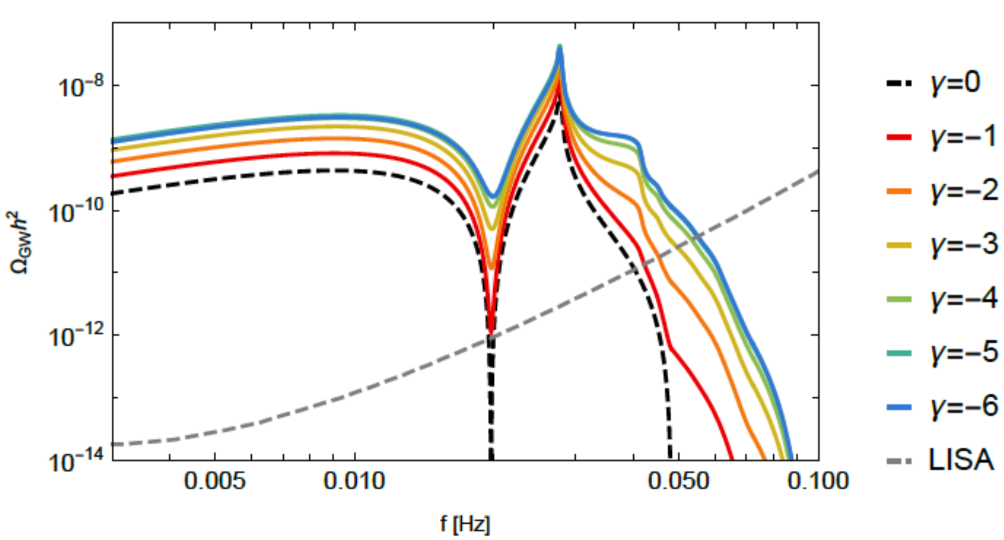


R. Inui et al., arXiv:2411.07647

**logarithmic non-Gaussianity**

$$\hat{\zeta}(r) = -\frac{1}{\gamma}\ln\Big(1 - \gamma\hat{\zeta}_g(r)\Big)$$

# ② LVK O3 constraint on PBH mergers

## Early binary formation

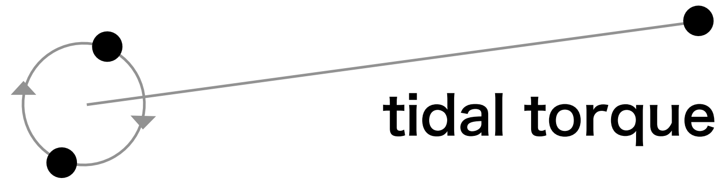


T. Nakamura et al. ApJ 487, L139 (1997)
K. Ioka et al., PRD 58, 063003 (1998)
M. Sasaki et al. PRL 117, 061101 (2016)

## Late binary formation

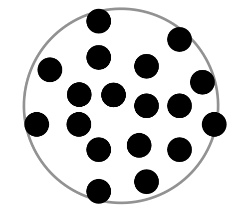

dynamical capture in a cluster

G. D. Quinlan, S. L. Shapiro, ApJ 343, 725 (1989)
H. Mouri, Y. Taniguchi, ApJ 566, L17 (2002)
S. Bird et al. PRL 116, 201301 (2016)
S. Clesse, J. García-Bellido, PDU 10 002 (2016)

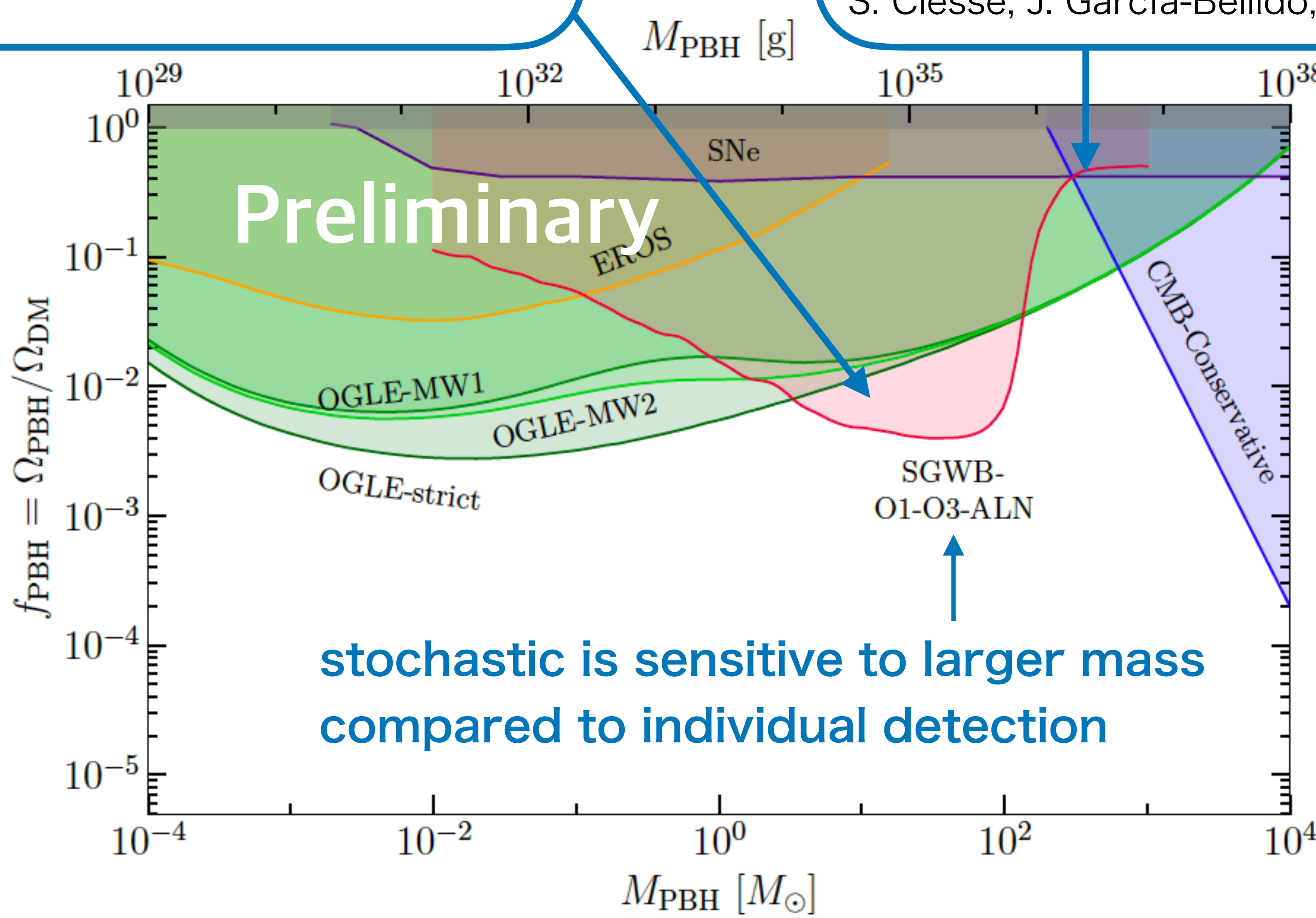


stochastic is sensitive to larger mass compared to individual detection

Monochromatic mass function is assumed

T. Boybeyi, S. Clesse, SK, M. Sakellariadou, in preparation

# Note on the merger rate modeling

## ② PBH mergers   Lots of uncertainties in theoretical prediction!

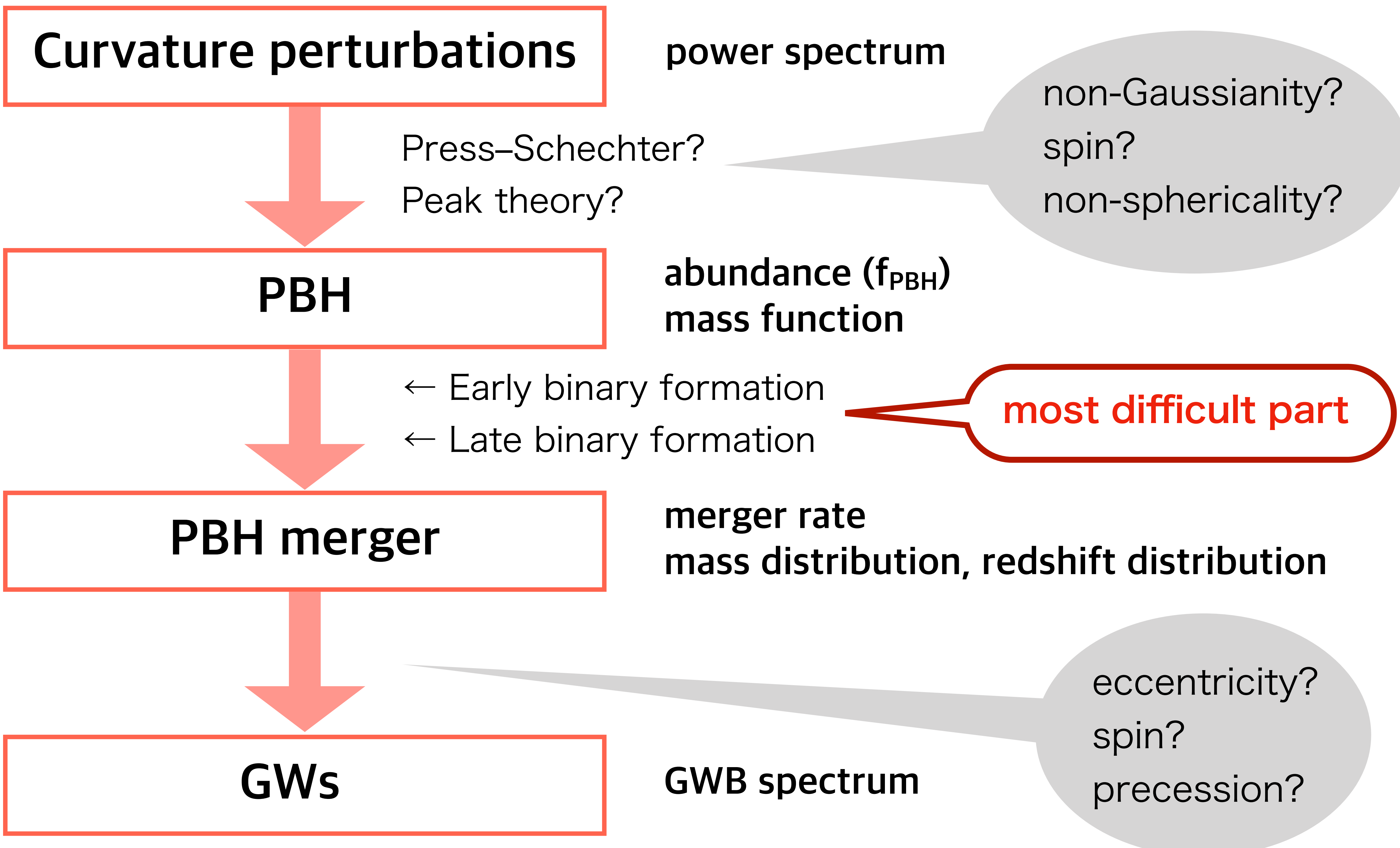

# Theoretical uncertainties

## Early binary formation

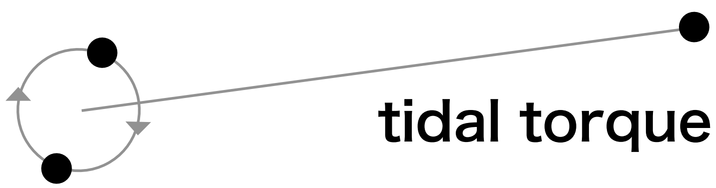


T. Nakamura et al. ApJ 487, L139 (1997)
K. Ioka et al., PRD 58, 063003 (1998)
M. Sasaki et al. PRL 117, 061101 (2016)

**merger rate**

$$R_{\rm EB} = \frac{1.6\times 10^6}{{\rm Gpc}^3{\rm yr}} \times \underline{f_{\rm sup}(m_1, m_2, f_{\rm PBH})} f_{\rm PBH}^{53/37} f(m_1) f(m_2) \times \left(\frac{t}{t_0}\right)^{-34/37} \left(\frac{m_1+m_2}{M_\odot}\right)^{-32/37} \left[\frac{m_1 m_2}{(m_1+m_2)^2}\right]^{-34/37}$$

**$f_{\rm sup}$: suppression factor**

Raidal et al., JCAP 1902, 018 (2019)

takes into aaccount binary disruption by
- local matter inhomogeneities
- initial Poisson fluctuations

PBH clusters
→ modification of semi-major axis and eccentricity

- Tested by N-body simulation, but picture may completely change for wide mass function.
- Simulation is difficult for wide mass range.

# Theoretical uncertainties

## Late binary formation

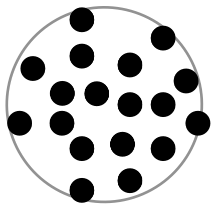

**dynamical capture in a cluster**

G. D. Quinlan, S. L. Shapiro, ApJ 343, 725 (1989)
H. Mouri, Y. Taniguchi, ApJ 566, L17 (2002)
S. Bird et al. PRL 116, 201301 (2016)
S. Clesse, J. García-Bellido, PDU 10 002 (2016)

**merger rate**

$$R_{\rm LB} \approx \underline{R_{\rm clust}} f_{\rm PBH}^2 f(m_1) f(m_2) \frac{(m_1+m_2)^{10/7}}{(m_1 m_2)^{5/7}} {\rm yr}^{-1}{\rm Gpc}^{-3}$$

**$R_{\rm clust}$: clustering factor**

$$R_{\rm clust} \approx 3.6 h^4 \left(\frac{\Omega_{\rm DM}}{0.25}\right)^2 \left(\frac{\delta_{\rm loc}}{10^8}\right) \left(\frac{v_0}{10~{\rm km/s}}\right)^{-11/7}$$

estimated by a very simplified picture

- kicks
- dynamical friction
- What is the cluster density?
  How many?
  distribution?
- Picture changes for wide mass function

→ need to follow BH dynamics throughout the history of the universe

# Individual binary search

# Searching primordial black holes

Detection of BH with < ∼1M⊙ can be a strong evidence of primordial origin

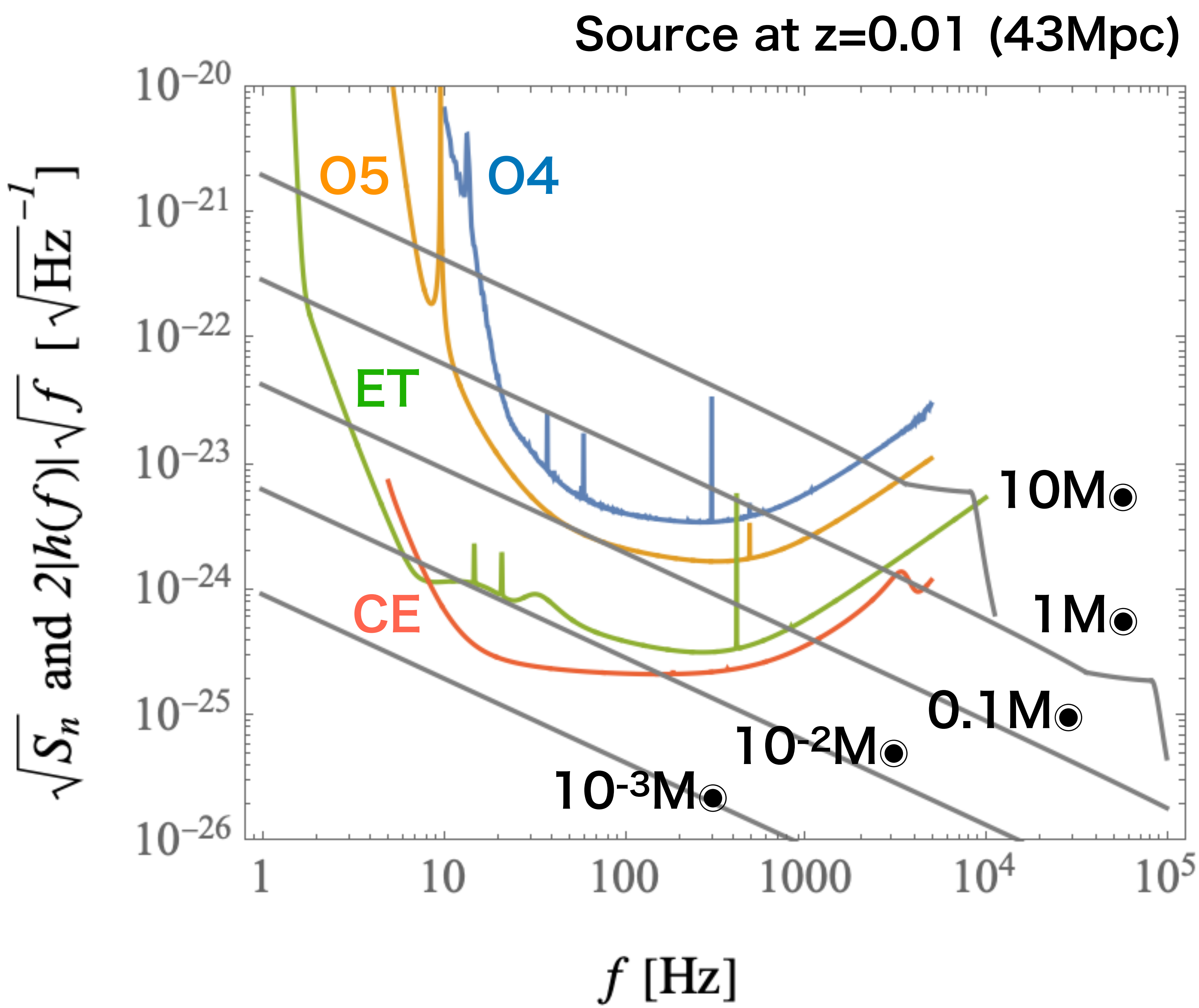

# Search method

**Chirp time (at Newtonian order)**

$$\tau_0 = \frac{5}{256} M^{-5/3} (\pi f_0)^{-8/3} \eta^{-1}$$

Total mass: $M = m_1 + m_2$

Symmetric mass ratio: $\eta = \frac{m_1 m_2}{(m_1 + m_2)^2}$

Lowest frequency: $f_0$

## 0.2 - 2 M☉ Subsolar mass search

LVK collaboration, PRL 121, 231103 (2018); PRL 123, 161102 (2019);
PRL 129, 061104 (2022); arXiv:2212.01477

Nitz & Wang, ApJ, 915, 54 (2021)

Phukon et al., arXiv:2105.11449

Morrás et al., PDU 42, 101285 (2023)

→ compact binary coalescence (CBC) search

## $10^{-7}$ - 0.2 M☉ Planetary mass search

Miller et al., PDU 32, 100836 (2021)

Miller et al., PRD 105, 062008 (2022)

→ continuous wave (CW) search

# Planetary mass BH constraints

LVK collaboration, PRD 106, 102008 (2022)

## Continuous wave (CW) search

Initial target: spinning neutron star with mass asymmetry

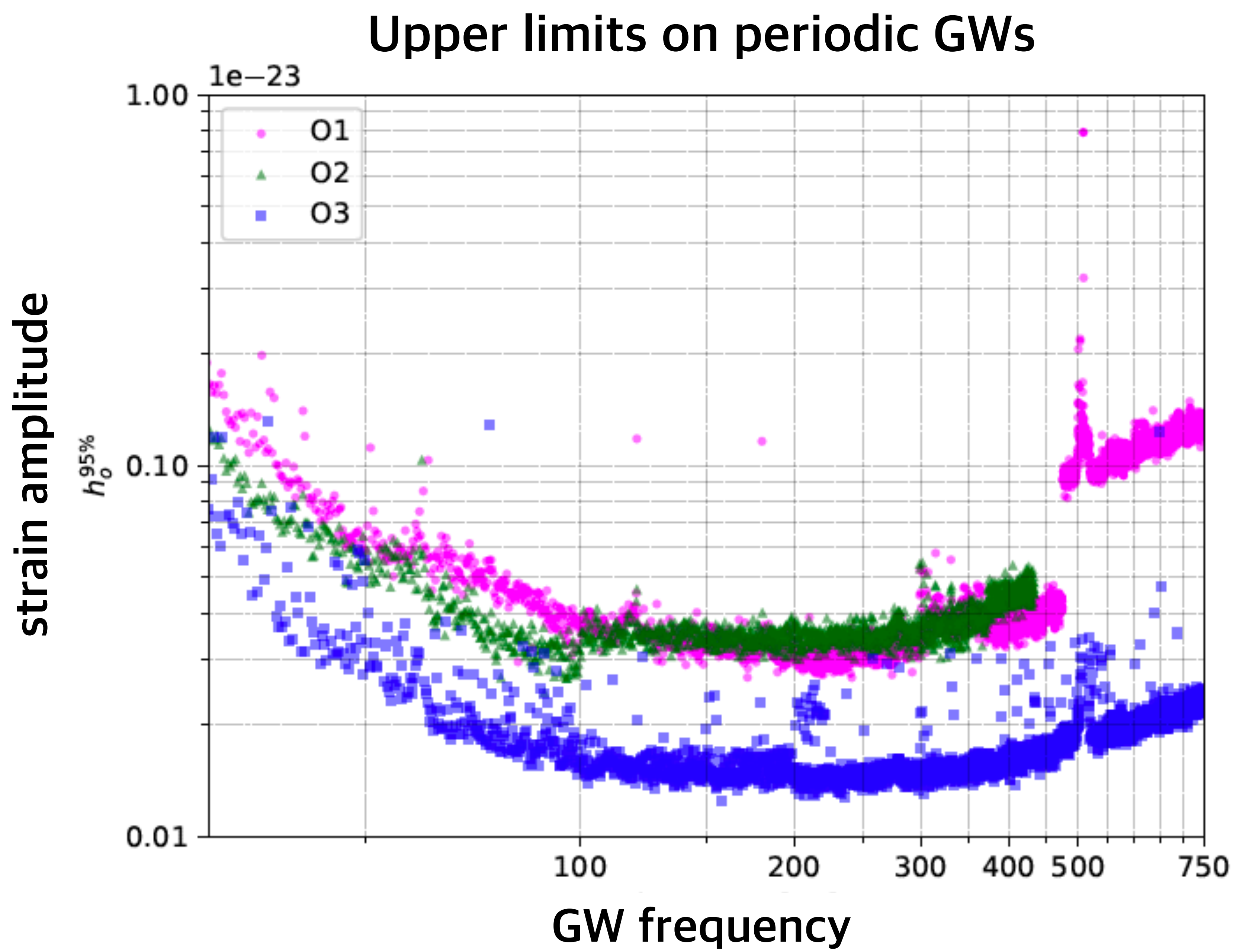


→ can be used to constrain small mass PBH binaries with small frequency change

# Constraints from CW search

Miller et al., PDU 32, 100836 (2021)
PRD 105, 062008 (2022)

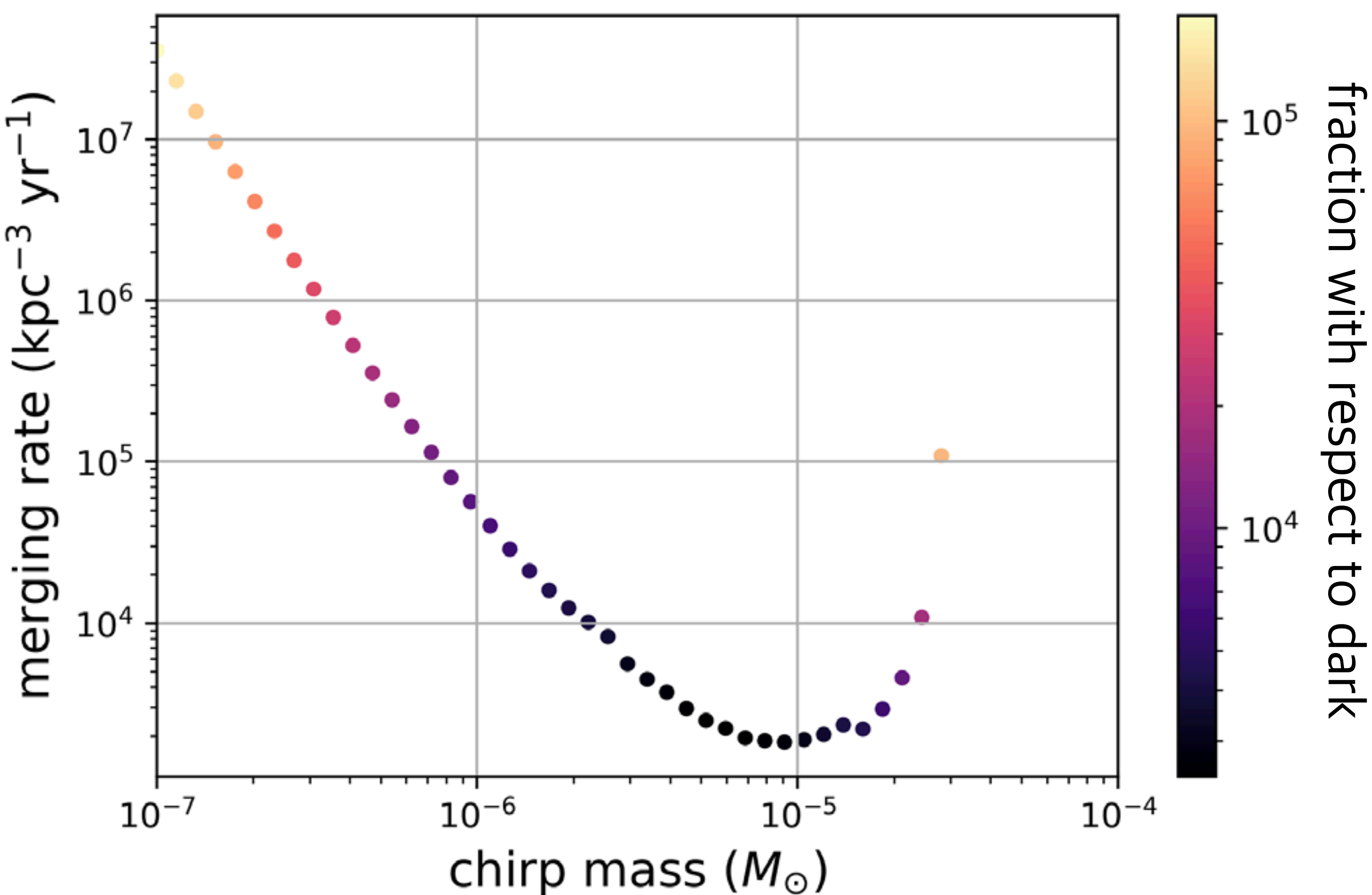


strain amplitude is too small | $\dot{f}$ is too large

**Frequency evolution**

$$\dot{f}_{gw} = \frac{96}{5}\pi^{8/3}\left(\frac{G\mathcal{M}}{c^3}\right)^{5/3} f_{gw}^{11/3}$$

**Powerflux pipeline**

→ searched periodic signal allowing spin-up of $\dot{f} \leq 1.00 \times 10^{-9}$ Hz/s

# Let us explore $> 10^5 M_\odot$

## Application of Viterbi algorithm

### Step-by-step scan for most probable signal location

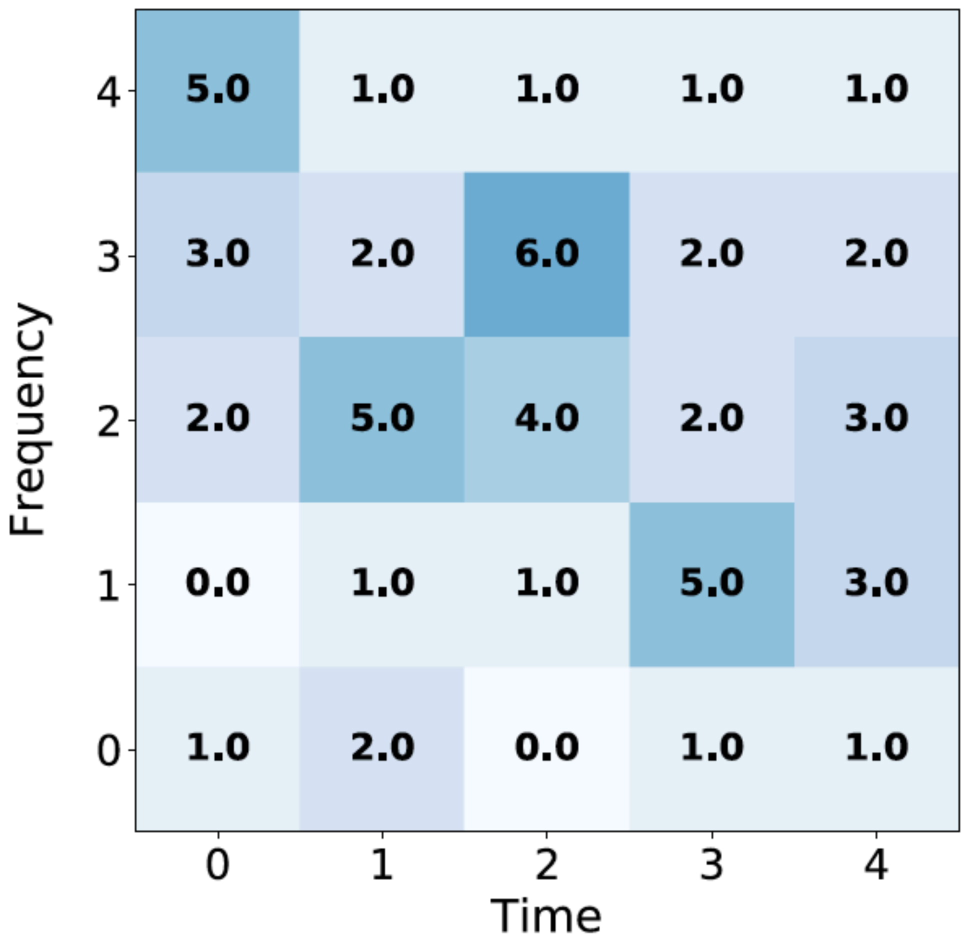


(a) The input data

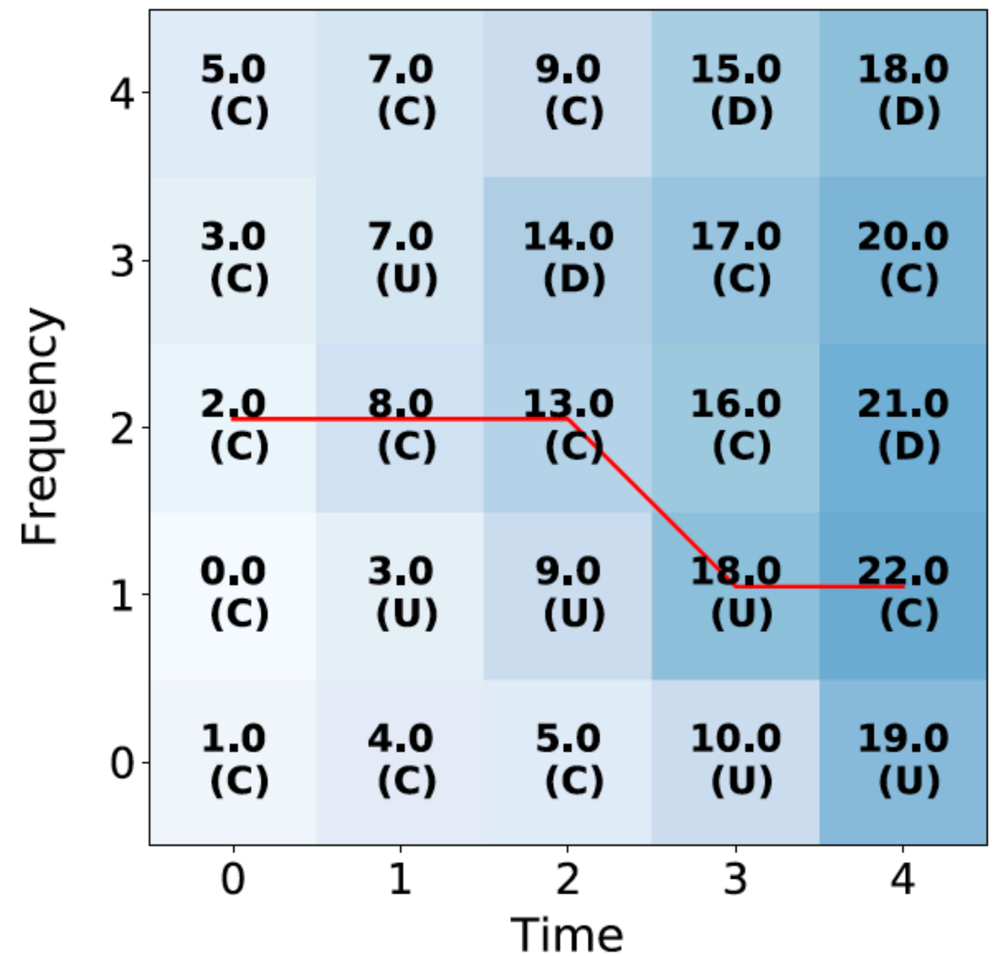


(b)The log-probabilities, jumps, and most probable path

**amplitude excess in the f-t plane**

Figure from Bayley et al. PRD 100, 023006 (2019)

G. Alestas et al. (+SK), PRD 109, 123516 (2024)

# Planetary mass search

Already used in CW search

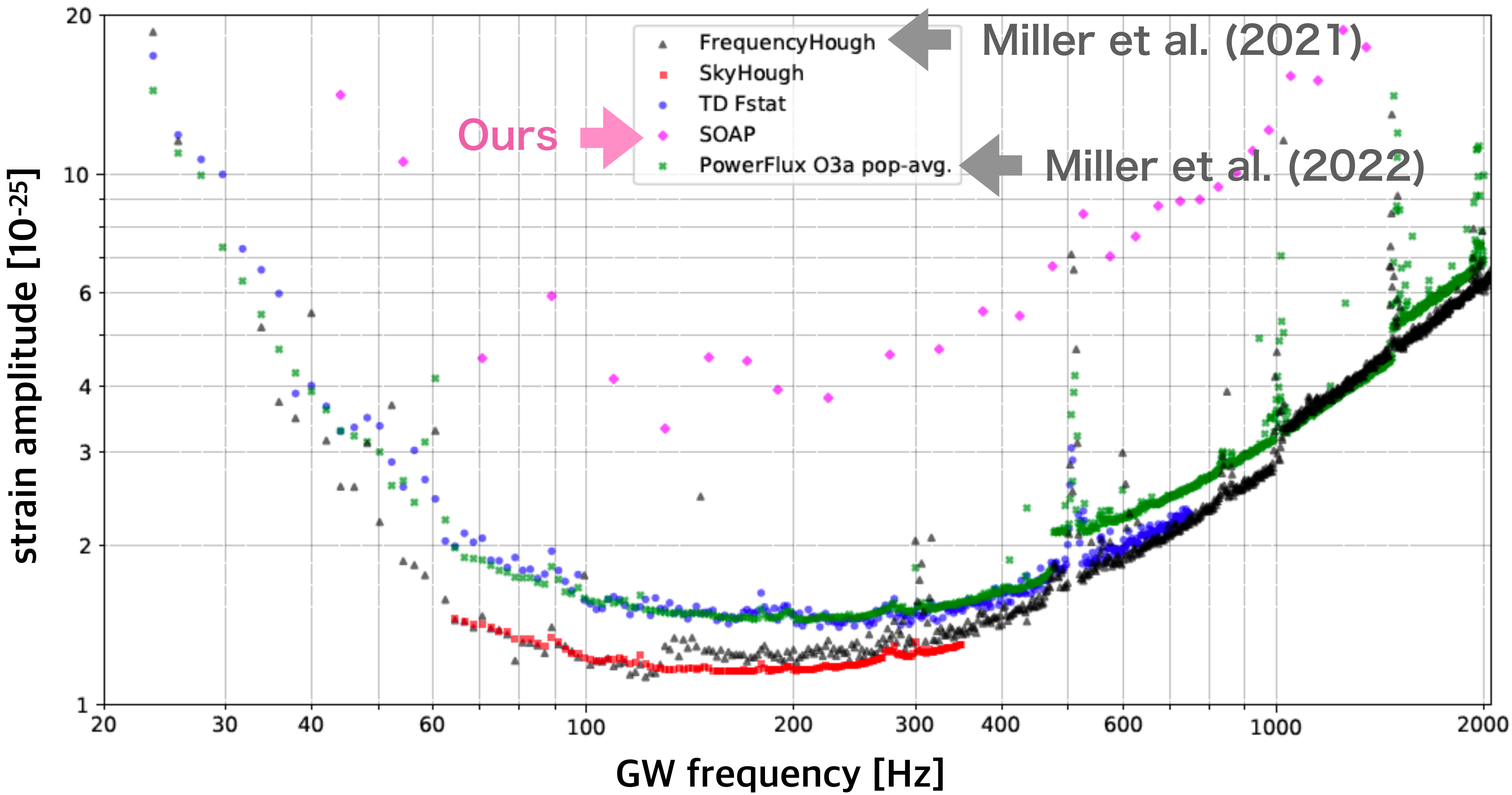


Not very sensitive, but fast and agnostic

# Search method

Signal duration is large when BH mass is small

Chirp time (at Newtonian order)

$$\tau_0 = \frac{5}{256} M^{-5/3} (\pi f_0)^{-8/3} \eta^{-1}$$

→ We divide the data into optimal length and perform SFT

SFT: short Fourier transform

Example: Chirp signal for NS binary

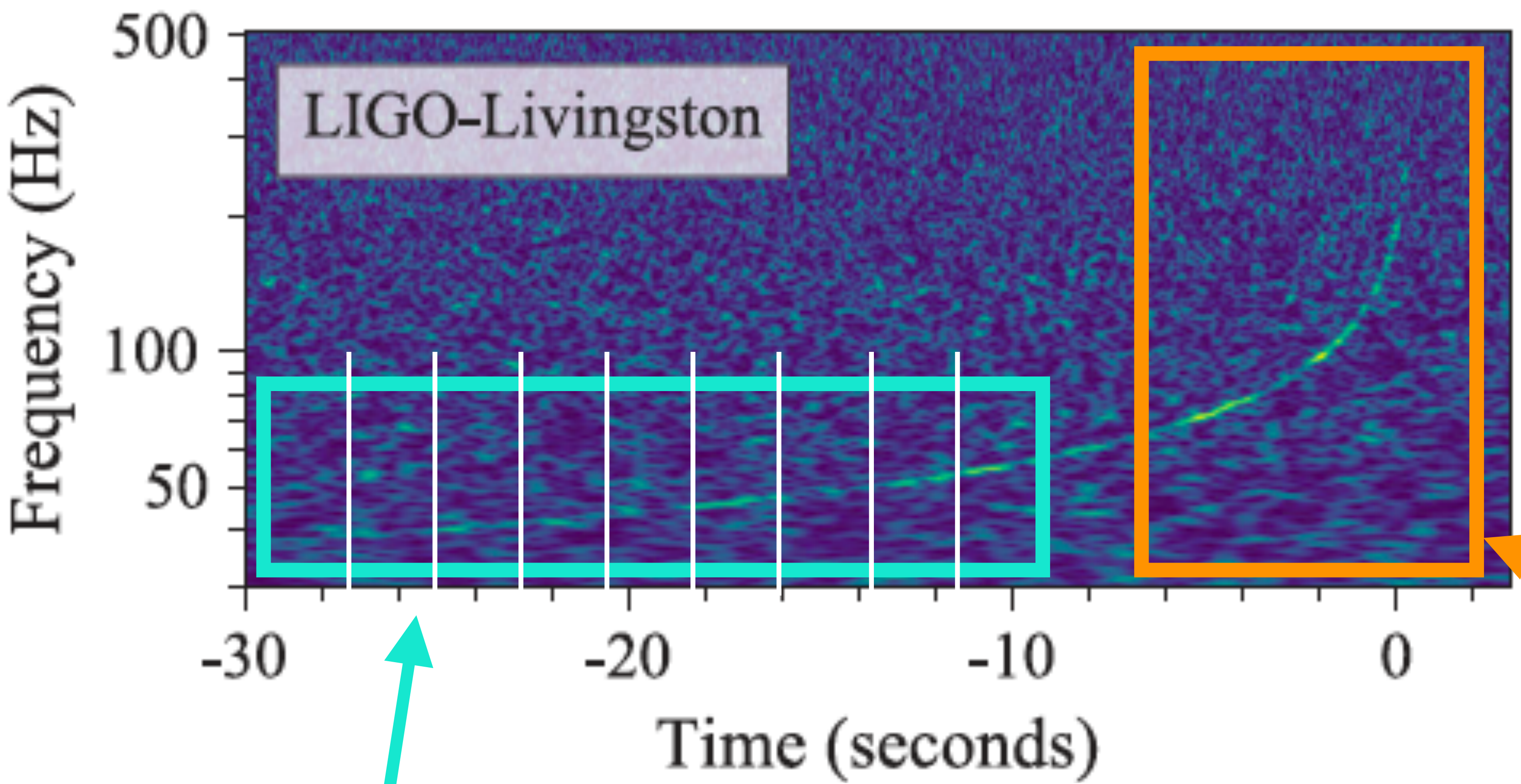


We don't observe this part if < $1M_\odot$

We are interested in slowly evolving part

# Search method

When $\dot{f}$ is relatively large, the signal do not stay in one frequency bin

Frequency evolution

$$\dot{f}_{gw} = \frac{96}{5}\pi^{8/3}\left(\frac{G\mathcal{M}}{c^3}\right)^{5/3} f_{gw}^{11/3}$$

→ We have to divide the data into optimal length

Example: Chirp signal for NS binary

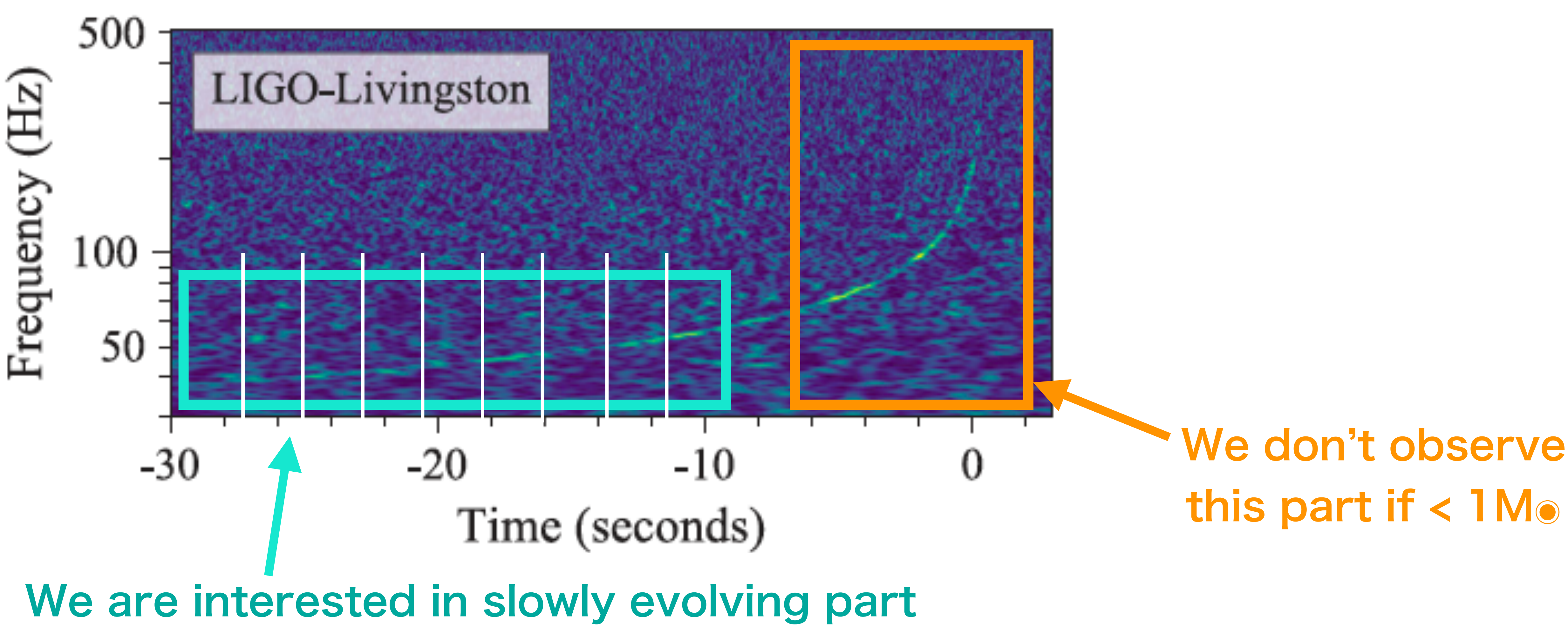

# Optimal SFT length

<u>SFT to maximize detection efficiency</u>

condition: signal has to stay in a single frequency bin of the SFT

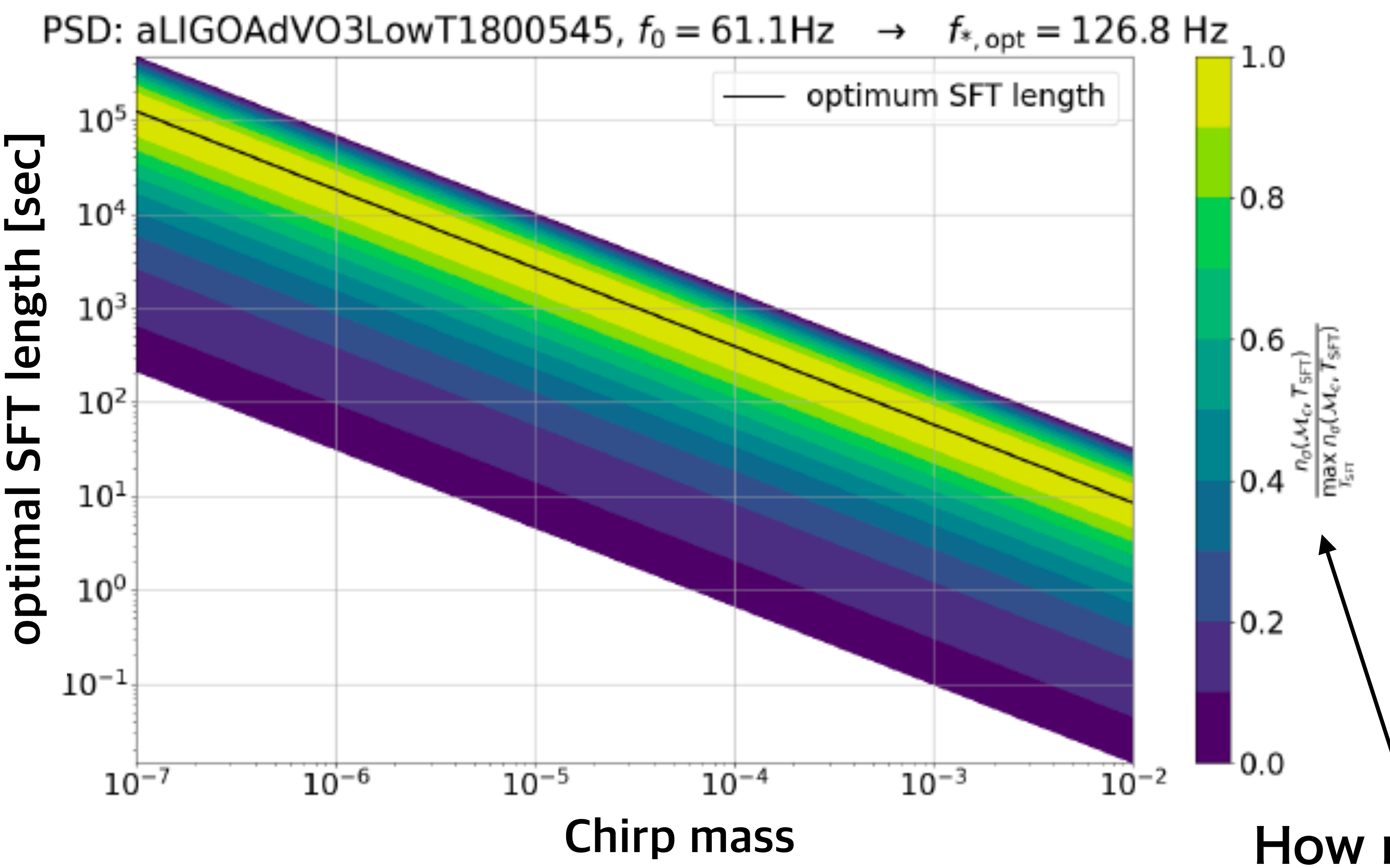


How much it loses SNR
if we use different length

G. Alestas et al. (+SK), PRD 109, 123516 (2024)

# Working example

O3 Gaussian noise is assumed

$$[\mathcal{M}_c, d_L] = [10^{-2} M_\odot, 147\mathrm{Kpc}]$$

<u>Injeccted signal</u>

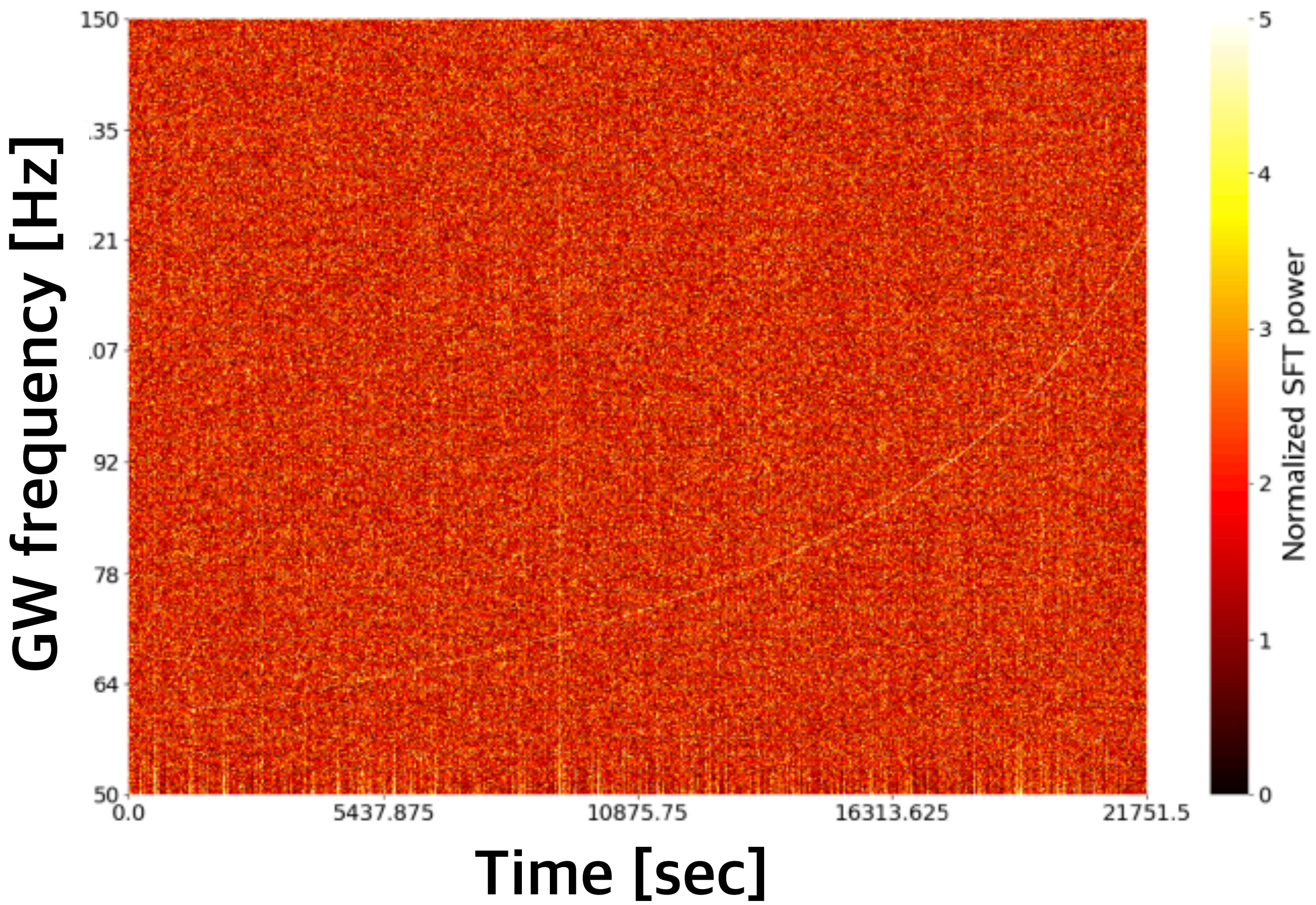


<u>Recovery by Viterbi</u>

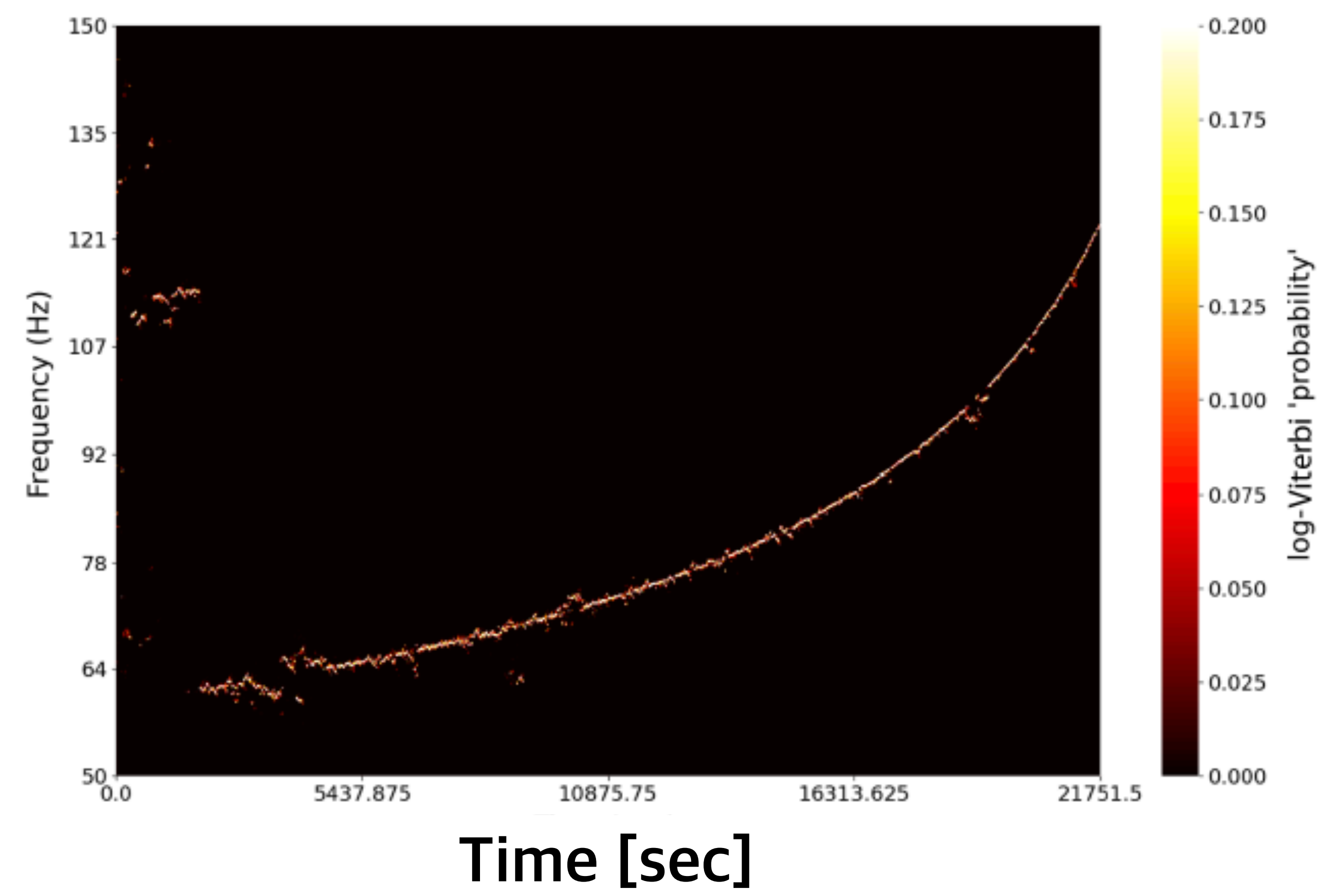


G. Alestas et al. (+SK), PRD 109, 123516 (2024)

# Sensitivity

for equal mass binary

Solid: analytic estimation
Dots: simulation

**Signal-to-noise ratio**

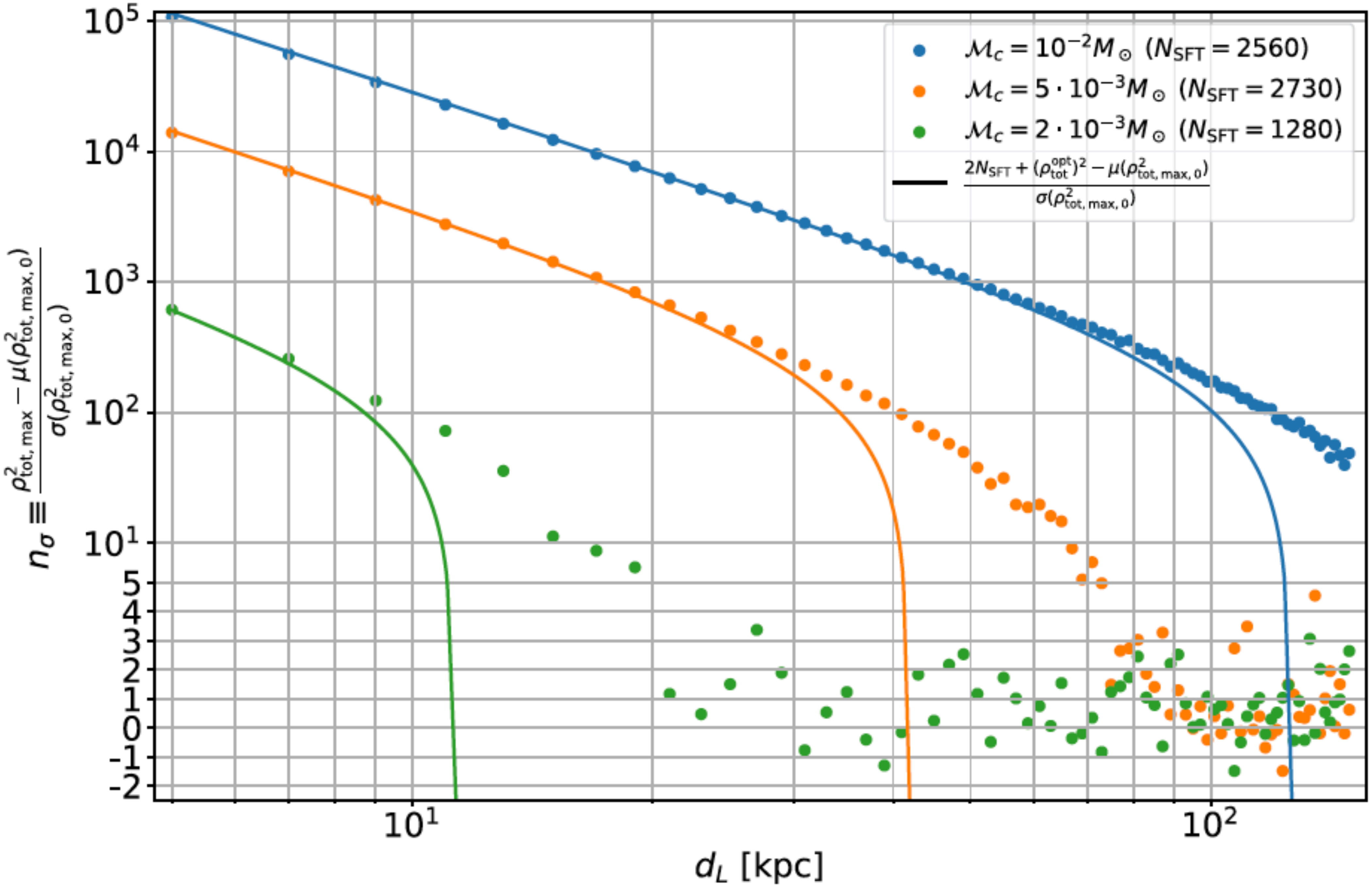


**Distance**

G. Alestas et al. (+SK), PRD 109, 123516 (2024)

# Summary

## Gravitational wave is a unique probe of primordial black hole scenarios

Stochastic search

- **Inui et al. (+SK) JCAP 05, 082 (2024), arXiv: 2311.05423**
  We have provided constraint on scalar induced GWs using LVK O3 data, by taking into account the effect of non-Gaussianity in curvature perturbations.

- **Boybeyi et al. (+SK) in preparation**
  We have provided constraint on PBH binaries using LVK O3 data by considering both early and late binary formation.

Continuous wave search

- **Alestas et al. (+SK) PRD 109, 123516 (2024)**
  We have formulated a method to search planetary mass ($10^{-2}$ - $10^{-5}M_\odot$) PBH with the application of Viterbi algorithm.

# Subsolar mass search

## Matched filtering

Data — Template = expected waveform

$$\rho^2 = \frac{\left[\int_{f_{\rm ini}}^{\infty} df \frac{\tilde{h}(f)\tilde{h}_t^*(f) + \tilde{h}^*(f)\tilde{h}_t(f)}{S(f)}\right]^2}{\int_{f_{\rm ini}}^{\infty} df \frac{|\tilde{h}_t(f)|^2}{S(f)}}$$

Noise

Normalization factor

Assuming $\tilde{h}(f) = \tilde{h}_t(f)$

**Signal-to-noise ratio (SNR)**

$$\rho^2 = \int_0^{\infty} \frac{(2|\tilde{h}(f)|\sqrt{f})^2}{S_n(f)} \mathrm{d}\ln(f)$$

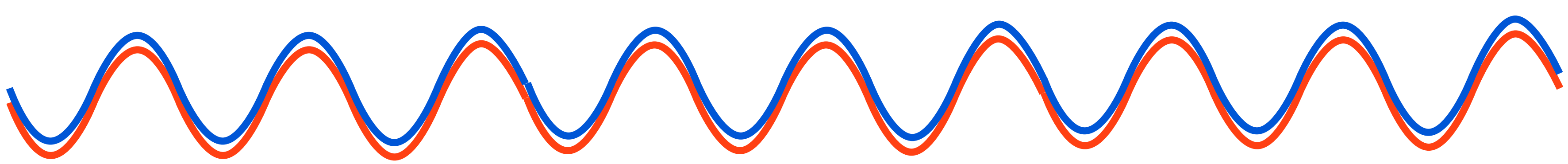

→ matched: SN is maximized

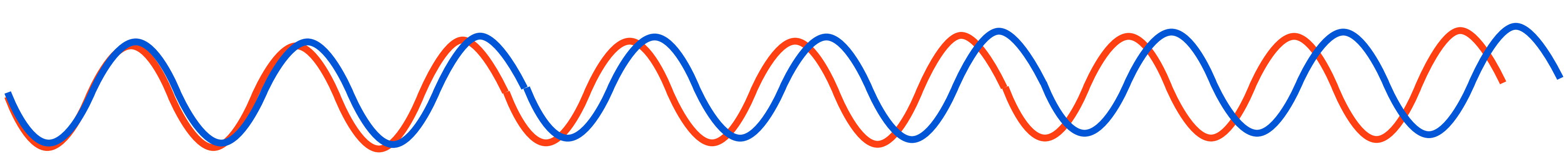

→ mismatch: SN is reduced

# Template bank

How do we find the correct template?
→ We simply try many and search for parameter values that maximize the SNR.

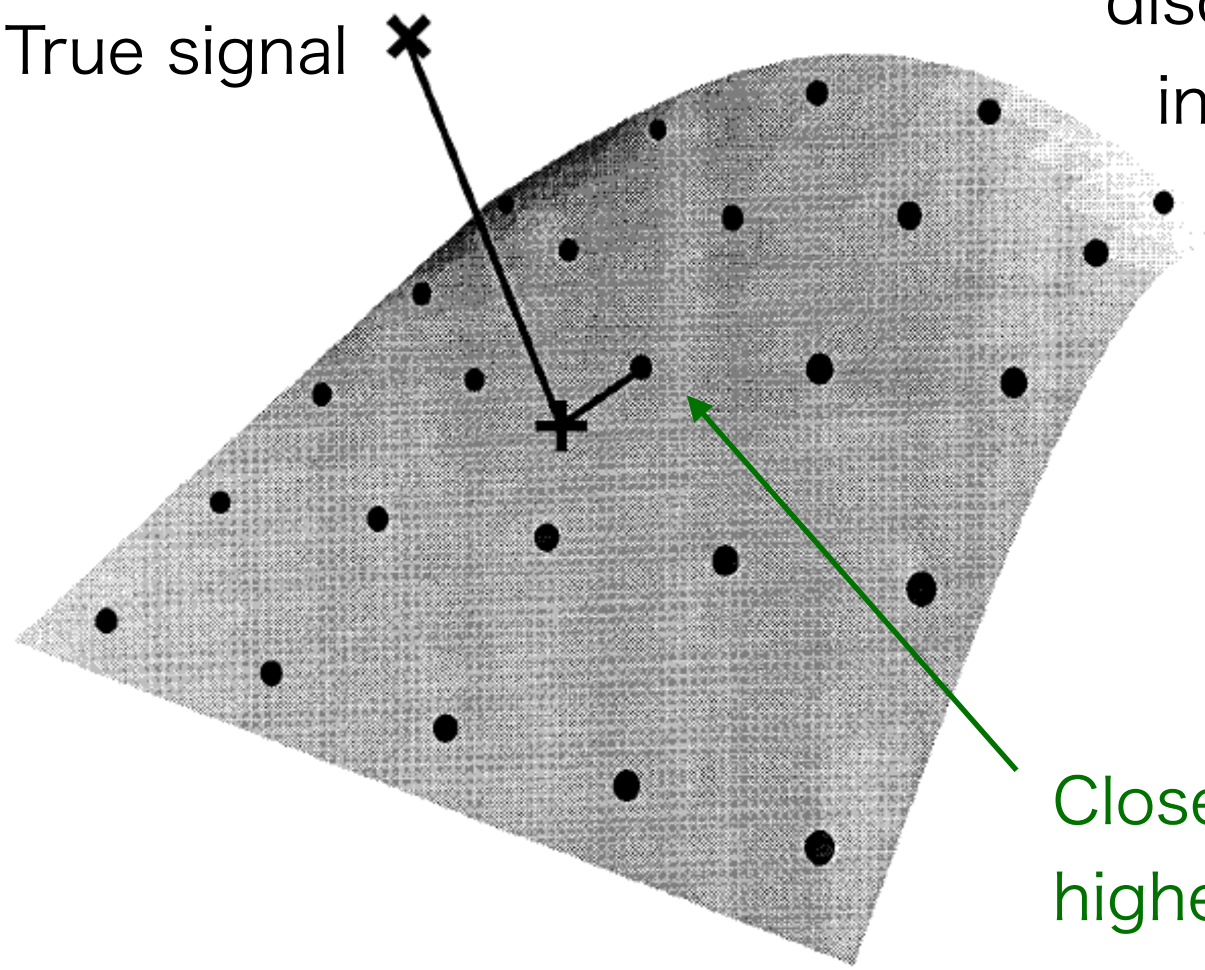


Typically, the discreteness of the template bank is selected in a way that ensures the loss of SNR is less than 3%

Figure from Owen, PRD 53, 6749 (1996)

# Challenge in subsolar mass search

**Low mass event continues long time and has more oscillation cycles.**

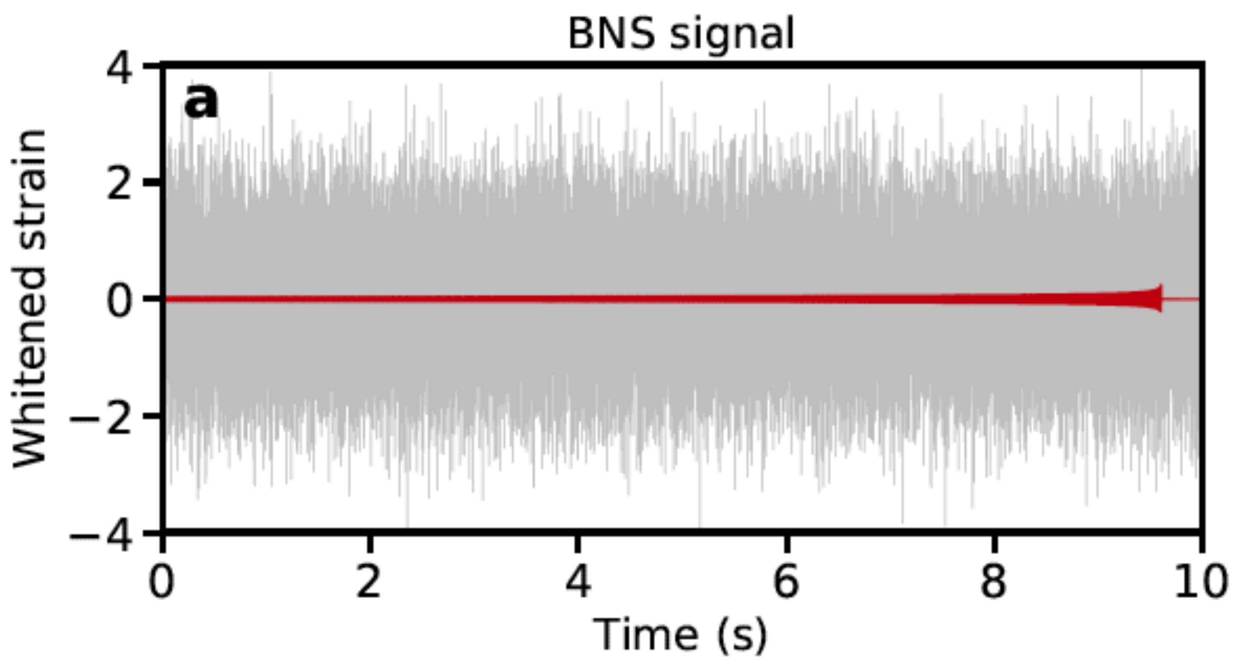


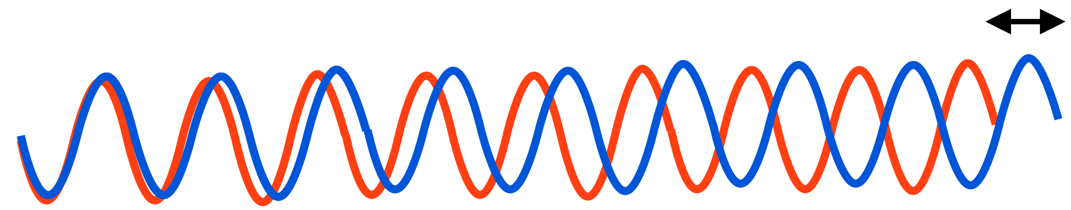

→ sensitive to small phase shift by variation of parameters

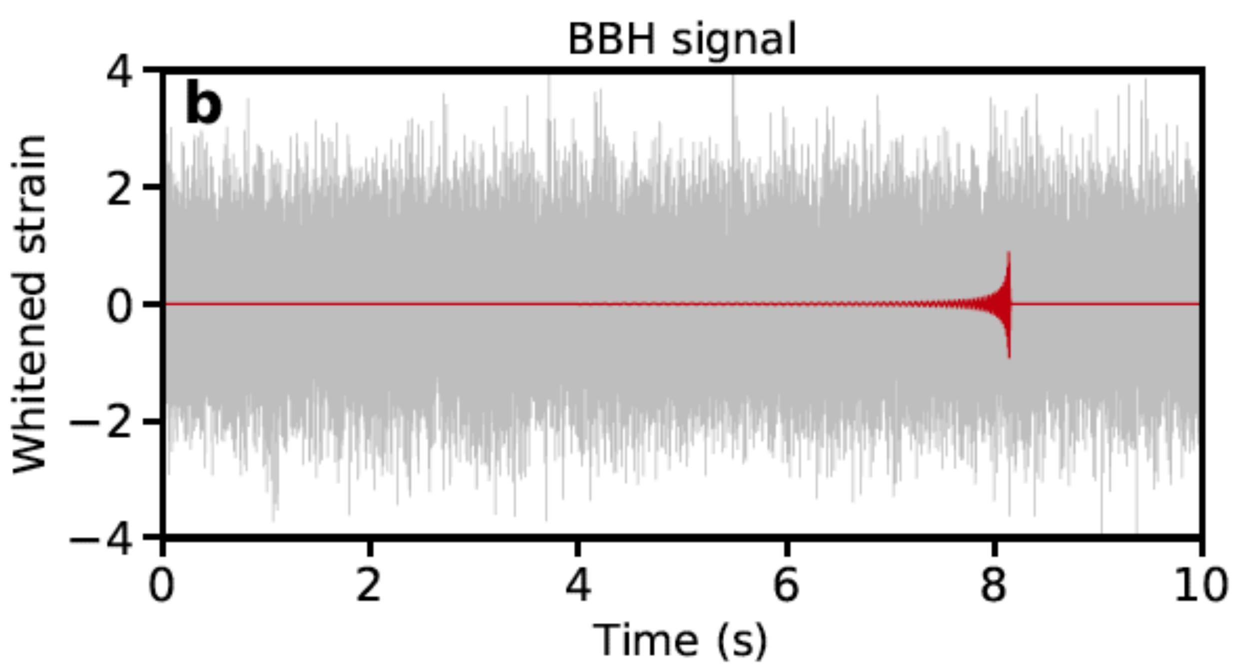


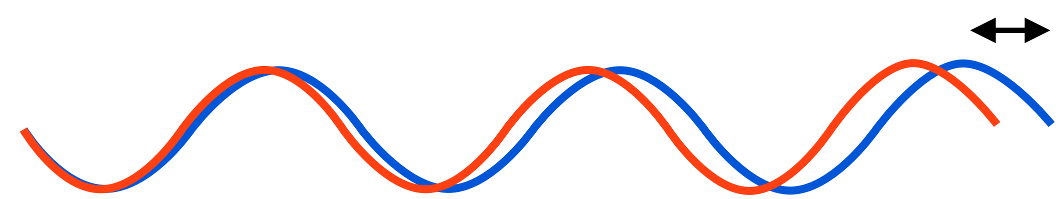

→ insensitive to small phase shift

→ **need to decrease the grid size of the template bank**

**→ more computation time**

Figure from Krastev, PLB 803, 135330 (2020)

# Challenge in subsolar mass search

Low mass event requires fine gridding to avoid mismatch.

Template used in O1 CBC search

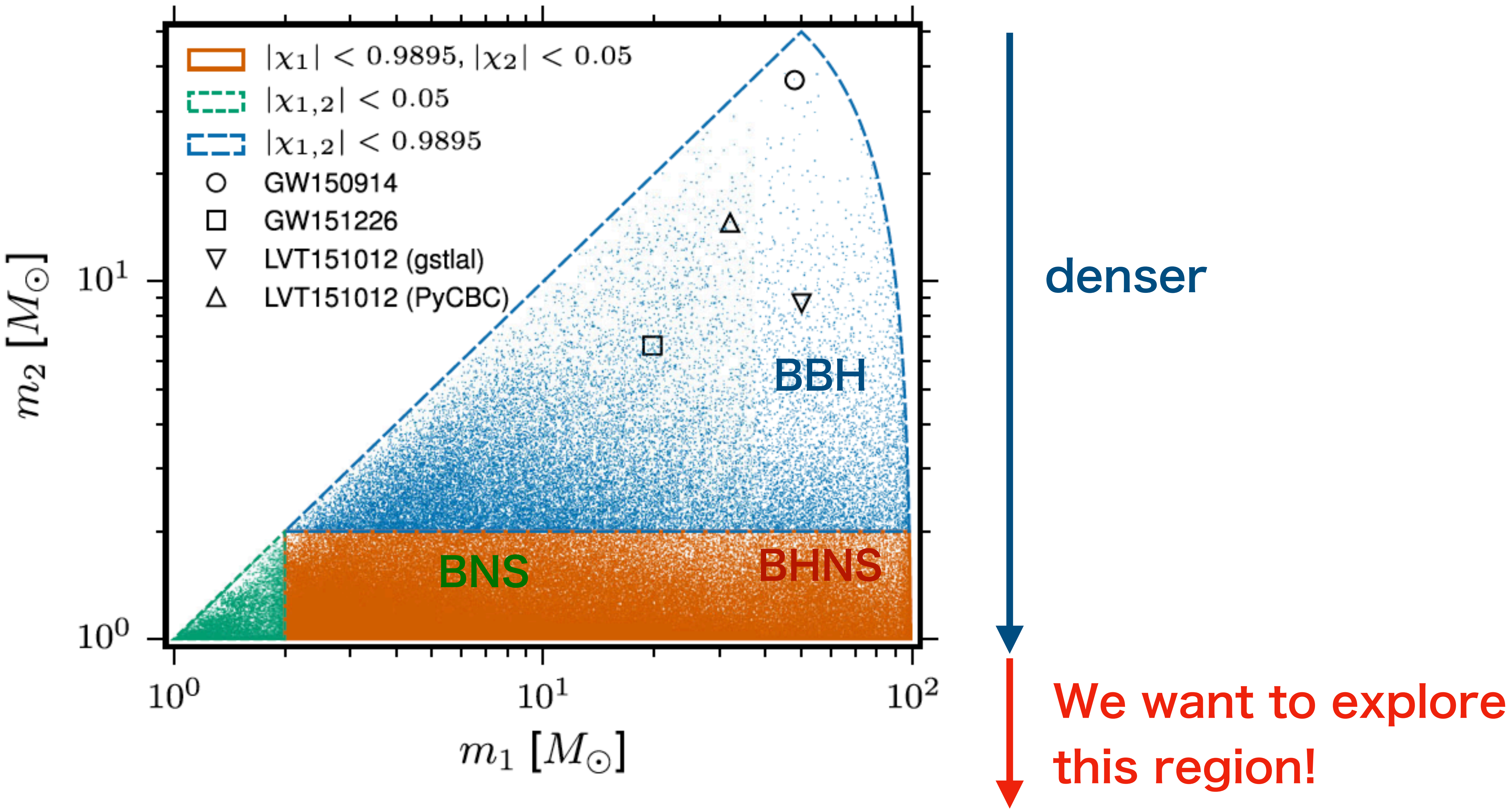


LVK collaboration, PRX 6, 041015 (2016)

# Remedy(?): cutting low frequency

Magee et al. PRD 98, 103024 (2018)

Number of template: $N \propto m_{\min}^{-8/3} f_{\min}^{-8/3}$

→ Increasing $f_{min}$ helps to reduce computation time, but it reduces the SNR

Volume ∝ $SNR^3$

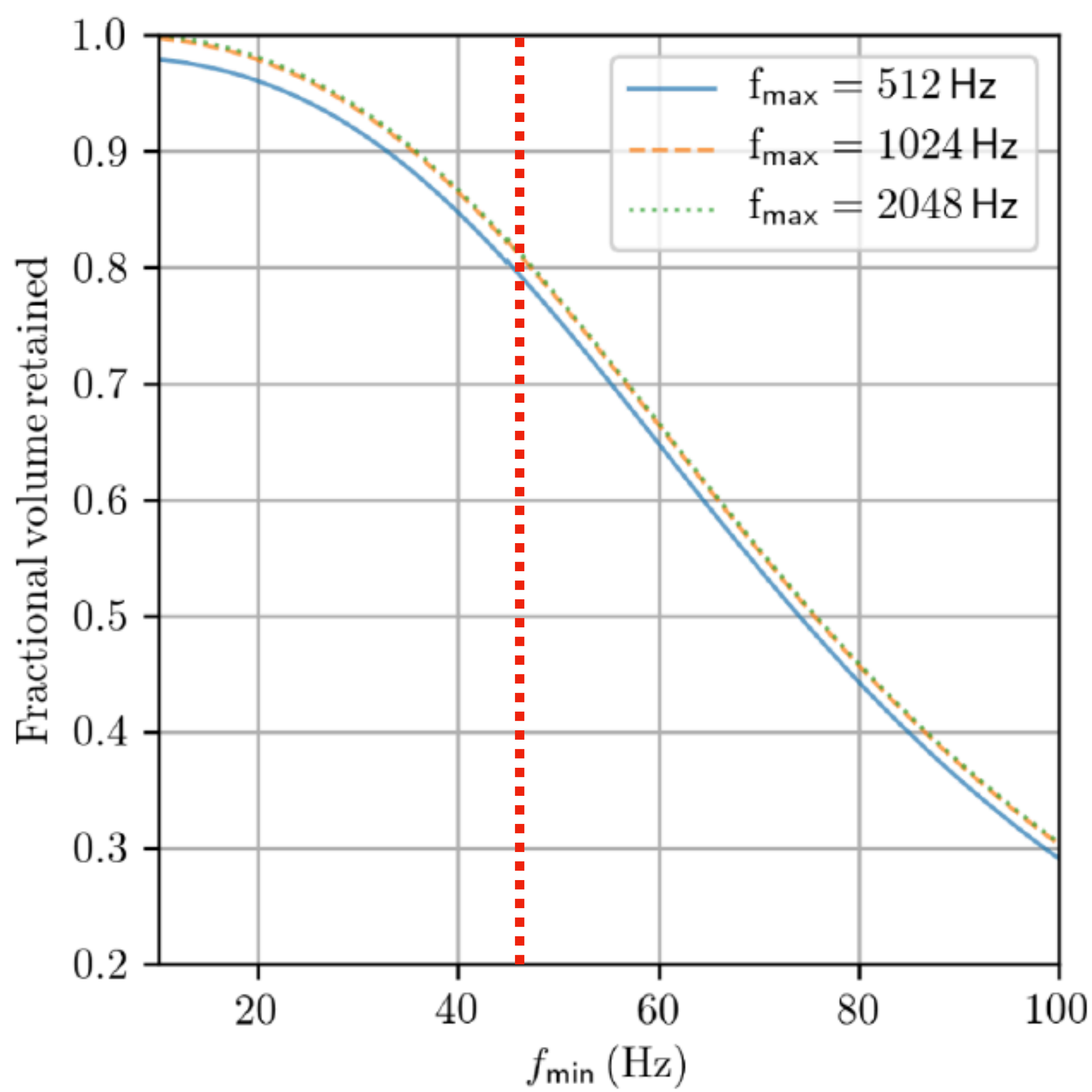


← $f_{min}$ = 45Hz is commonly used in LVK search, allowing 20% loss in volume

# Sub-solar mass search in LVK

**O3b** $f_{\min} = 45\text{Hz}$

LVK collaboration, arXiv:2212.01477

search range: $m_1 \in [0.2,\ 10\ ]\ M_\odot$

$m_2 \in [0.2,\ 1.0\ ]\ M_\odot$

$0.1 < q < 1.0 \qquad q \equiv m_2/m_1$

$\chi_{1,2} < 0.9$

cf. number of templates
O1: 500332
O2: 992461
O3: ?

**Triggers with FAR < 2 yr$^{-1}$**

| FAR [yr$^{-1}$] | Pipeline | GPS time | $m_1$ [$M_\odot$] | $m_2$ [$M_\odot$] | $\chi_1$ | $\chi_2$ | H SNR | L SNR | V SNR | Network SNR |
|---|---|---|---|---|---|---|---|---|---|---|
| 0.20 | GstLAL | 1267725971.02 | 0.78 | 0.23 | 0.57 | 0.02 | 6.31 | 6.28 | - | 8.90 |
| 1.37 | MBTA | 1259157749.53 | 0.40 | 0.24 | 0.10 | −0.05 | 6.57 | 5.31 | 5.81 | 10.25 |
| 1.56 | GstLAL | 1264750045.02 | 1.52 | 0.37 | 0.49 | 0.10 | 6.74 | 6.10 | - | 9.10 |

rate

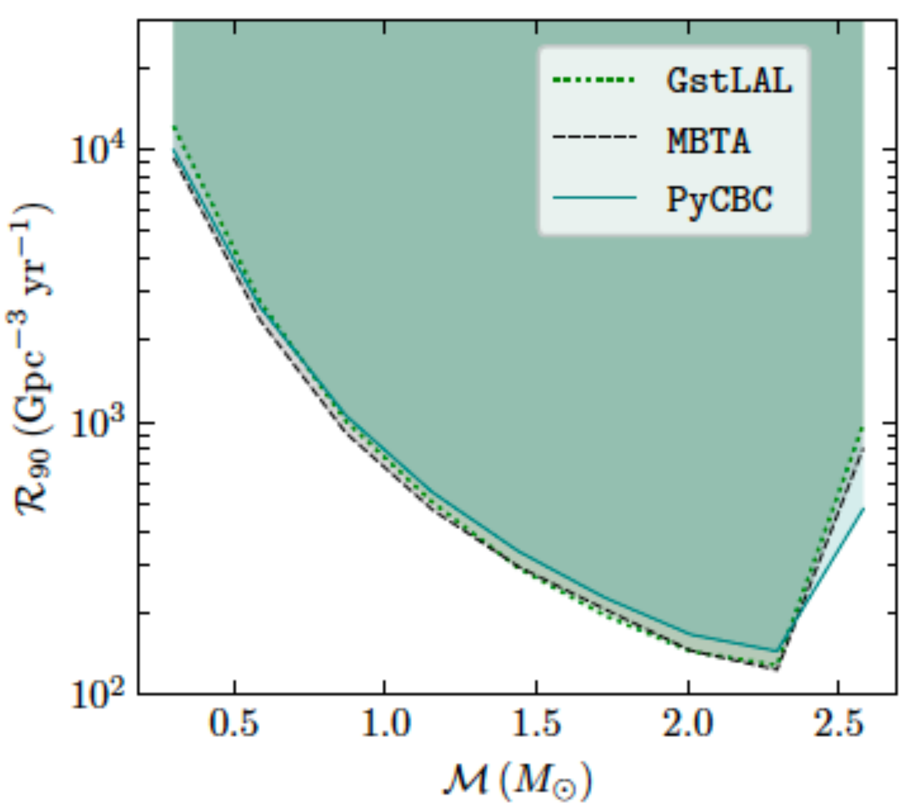


chirp mass

Assumption:
early binary formation
Sasaki et al. PRL 117, 061101 (2016)
Raidal et al. JCAP 02, 018 (2019)

PBH fraction

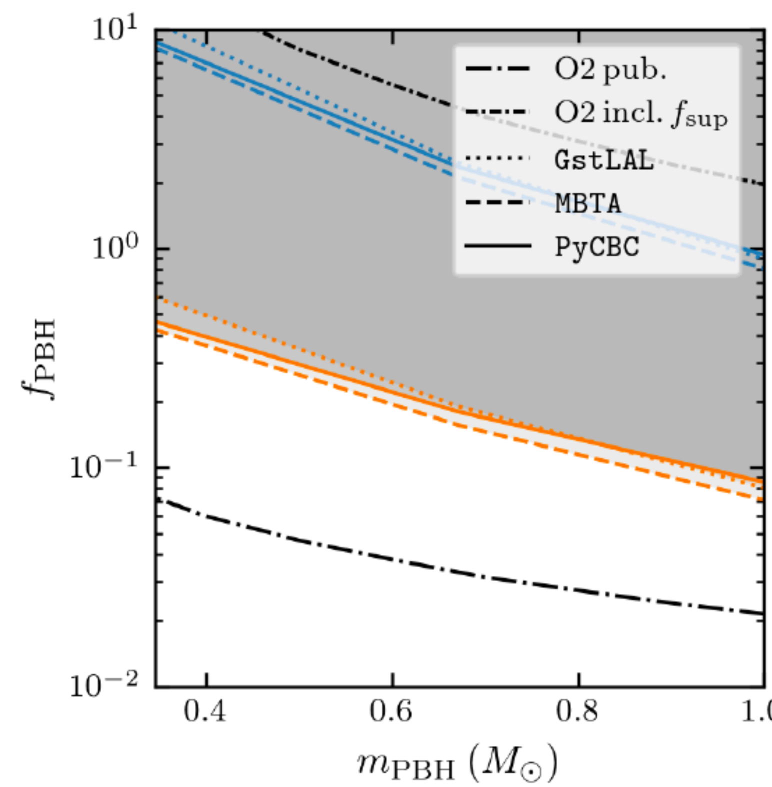


PBH mass

# Sub-solar mass search in LVK

**O2** Extended search of O2 data (allowing large mass ratio)

**Triggers with FAR < 2 $yr^{-1}$**

Phukon et al., arXiv: 2105.11449

| FAR [$yr^{-1}$] | ln $\mathcal{L}$ | UTC time | mass 1 [$M_\odot$] | mass 2 [$M_\odot$] | spin1z | spin2z | Network SNR | H1 SNR | L1 SNR |
|---|---|---|---|---|---|---|---|---|---|
| 0.1674 | 8.457 | 2017-03-15 15:51:30 | 3.062 | 0.9281 | 0.08254 | -0.09841 | 8.527 | 8.527 | - |
| 0.2193 | 8.2 | 2017-07-10 17:52:43 | 2.106 | 0.2759 | 0.08703 | 0.0753 | 8.157 | - | 8.157 |
| 0.4134 | 7.585 | 2017-04-01 01:43:34 | 4.897 | 0.7795 | -0.05488 | -0.04856 | 8.672 | 6.319 | 5.939 |
| 1.2148 | 6.589 | 2017-03-08 07:07:18 | 2.257 | 0.6997 | -0.03655 | -0.04473 | 8.535 | 6.321 | 5.736 |

reanalysis by
removing a glitch
extending $f_{min}$ to 20Hz
using more accurate waveform

→ SNR is reduced

Morrás et al., PDU 42, 101285 (2023)

| Parameter | IMRPhenomPv2 | IMRPhenomXPHM |
|---|---|---|
| Signal to Noise Ratio | $7.98^{+0.62}_{-1.03}$ | $7.94^{+0.70}_{-1.05}$ |
| Primary mass ($M_\odot$) | $4.65^{+1.21}_{-2.15}$ | $4.71^{+1.57}_{-2.18}$ |
| Secondary mass ($M_\odot$) | $0.77^{+0.50}_{-0.12}$ | $0.76^{+0.50}_{-0.14}$ |